NORTHERN ARIZONA UNIVERSITY

Lab of Landscape Ecology and Conservation Biology

FINAL REPORT

(30 September 2011)

For the project entitled:

Development of state-of-the-art tools and functionality for the Kaibab National Forest Monitoring Plan.

USFS-NAU Agreement # 09-CR-11030700-019

Submitted to:

The Kaibab National Forest

By:

Brett G. Dickson, Ph.D.

Principal Investigator

Recommended citation:

Dickson, B. G., A. D. Olsson, S. E. Sesnie, and M. A. Williamson. 2011. Development of state-of-the-art tools and functionality for the Kaibab National Forest Monitoring Plan. Final Report to the Kaibab National Forest. Lab of Landscape Ecology and Conservation Biology, Northern Arizona University, Flagstaff, AZ. 54pp.

School of Earth Sciences and Environmental Sustainability • Northern Arizona University
PO Box 5694 • Flagstaff, Arizona 86011-5694

Project overview

As part of an existing cost reimbursable agreement between the Kaibab National Forest (KNF) and the Lab of Landscape Ecology and Conservation Biology (LLECB) at Northern Arizona University, this final report encompasses two principal phases of work, iteratively defined in cooperation with Agency representatives: 1) the refreshing and refining of high spatial resolution digital data layers on forest structure for the purpose of developing a prototype "monitoring toolbox" and estimating change in conditions over time, and 2) the integration of these forest structure data layers into spatially explicit estimates of occupancy probability for songbirds on the KNF. The monitoring toolbox includes multiple refreshed (i.e., 2006, 2010) data products characterizing contemporary forest structure conditions, as well as a framework and template for future data refresh and analyses. Model results and estimates of occupancy for three Management Indicator Species demonstrate the utility of these forest structure data for informing ongoing wildlife monitoring and planning efforts on the KNF. These latter results were achieved in collaboration with the Grand Canyon Trust. Specifically, products from this report were designed to inform and refine the KNF Monitoring Plan matrix and Draft Environmental Impact Statement (DEIS), including an analysis of avifaunal occupancy, and to support effects analyses to be incorporated into the DEIS for silviculture and wildlife programs. The following sections detail each of the two completed phases of work. Future phases of work will build on the associated deliverables.

Developing a monitoring toolbox for the Kaibab National Forest Monitoring Plan: modeling forest structure and change.

BACKGROUND AND INTRODUCTION

The objective of this phase of work was to develop practical and defensible tools to monitor forest management activities and progress towards meeting Kaibab National Forest (KNF) planning and monitoring objectives, including changes in forest structural conditions. Freely available US Forest Service permanent Forest Inventory and Analysis (FIA) plots, Landsat Thematic Mapper (TM) imagery, and a USGS 30m digital elevation model (DEMs) were leveraged as the principal data sources for this work. FIA, TM, and DEM data were combined to develop medium resolution and multi-temporal digital forest structure data layers that cover the KNF, in addition to adjacent landscapes (Figure 1). For this work, we also focused on five different approaches to correct terrain and atmospheric effects on TM satellite imagery that were compared to uncorrected images used to predict forest structural parameters. Basal area (BA), stand density index (SDI), canopy cover (CC), mean tree height (HGT), trees per acre (TPA), and quadratic mean diameter (QMD) were the principal forest structural variables developed for evaluating model accuracy and consistency.

Remote sensing change analysis of pre- and post-treatment forest and landscape conditions requires comparable images from multiple dates. Medium resolution Landsat TM (30-m pixels and 7 spectral bands) images measure upwelling radiance from above the Earth's atmosphere that is sensitive to changes in the sun angle (e.g., time of day, time of year) and atmospheric conditions at the time of acquisition. To perform change analyses, images are typically corrected in order to make accurate comparisons consistent with conditions on the ground (Song et al. 2001). Common approaches to atmospheric correction are image-to-image calibration and the use of radiative transfer models. These methods are designed to enhance change detection while reducing mischaracterization areas left unchanged.

Image-to-image calibration is an empirical approach that treats one image as a reference and transforms ("normalizes") the other image based on an empirical relationship between pixels in the two images in areas where no change has occurred. So-called "invariant" pixels include sand, lava flows, deep water bodies or forest canopies. This empirical approach

requires no knowledge about atmospheric conditions or sun angle or azimuth for either date. Instead, it uses relatively invariant bright and dark land features across the spectrum of values in the scene. Automated techniques such as iteratively reweighted multivariate alteration detection (IR-MAD) search and identify 'no change' pixels in a way that removes observer bias and ensures invariant pixels that span the full spectrum are found (Canty 2010). Once 'no change' pixels have been identified, a model recalibrates target image pixels to the reference image to reduce the effect of atmospheric differences between image dates. In order to expand the analysis from two to three or more scenes, each new scene must be normalized to the reference image. In the end, each image has been altered to match the reference image.

Radiative transfer models treat each image independently and apply corrections according to local and regional assumptions about atmospheric effects on spectral reflectance recorded at the sensor. Each image and 'top of atmosphere' reflectance is converted to 'surface reflectance' by reducing the effect of atmospheric scattering and absorption. Sophisticated atmospheric models are contained within relatively easy-to-use software and utilize available image calibration data collected by satellite sensors to make appropriate corrections.

Topography also impacts image spectral reflectance values over time and space. For example, a gentle north-facing slope will reflect a smaller percentage of light on November 1 than on October 15. Unwarranted or severe changes in brightness produced by local hill slope and sun angle effects can result in different model predictions of forest structure characteristics. Illumination correction techniques are used to estimate sun illumination differences due to topography and correct shading of inordinately bright pixels. Illumination correction typically utilizes a digital elevation model (DEM) and correction coefficients "flatten" an image, lightening pixels where sun incident angles are lowest (e.g., north slopes) and darkening pixels where sun incident angles are highest (e.g., south slopes). Illumination correction requires an accurate DEM to adequately represent topographic conditions in order to correct illumination differences. Slight misalignment between DEM and TM pixels can result in dramatic overcorrection, particularly on the edges of high contrast terrain features (peaks, ridgelines, canyons).

Satellite images taken from different seasons provide contrasting vegetation conditions helpful for determining differences in forest composition and structure. Indeed, our previous work shows that models utilizing a leaf-on and leaf-off scene performed better than those based on a single image date. However, late fall sun angles enhance topographic shading and increase the likelihood of over- or under-correction in many image enhancement algorithms. Additionally, sun angles change more rapidly in the fall and spring, making the selection of anniversary scenes (i.e., images acquired from different years, but at or near the same calendar date) more critical because small differences in anniversary dates make greater differences in topographic illumination during fall and spring. The performance of multi-date models (e.g., models that utilize both leaf-on and leaf-off dates) must evaluated with respect to tradeoffs associated with the ability to accurately monitor forest changes and control for confounding image factors.

METHODS

STUDY AREA

The study area encompassed an area of over 6-million ha, including all of the KNF (Figure 1). This large extent allowed for a large number of Forest Inventory Analysis plots (*n* = 587) outside the KNF to enhance the predictive power of forest structural models.

LANDSAT TM IMAGE PROCESSING

The KNF is covered by three Landsat TM 'tiles' identified by path 37, row 34; path 37, row 35; and path 37, row 36. We acquired Landsat TM scenes for these tiles during leaf-on (September 19 and August 13) and leaf-off dates (October 21 and November 1) from 2006 and 2010. We mosaicked the scenes from each date together to make four mosaic scenes (leaf-on and leaf-off for 2006 and 2010, respectively) and cropped the mosaics to the study area. The four cropped mosaics were the basis for all further processing and served as the base-line "uncorrected" dataset. We used two different approaches to normalization to complement the uncorrected dataset: 1) an image-to-image normalization and 2) a physics-based atmospheric correction. We used IR-MAD to make the image-to-image normalization dataset, using the 2006

images as reference images and adapting the corresponding leaf-on and leaf-off images from 2010 to match the 2006 images (the "MAD" dataset). For the atmospheric correction, we used the Fast Line-of-sight Atmospheric Analysis of Spectral Hypercubes (FLAASH) algorithm in ENVI 4.7 to process the Landsat data to surface reflectance for each of the four mosaics (the "FLAASH" dataset). In addition to the three datasets described, we created three additional datasets wherein an illumination correction was applied before any image normalization. We used the C-corrected algorithm for illumination correction. The six datasets and their abbreviations are listed in Table 1.

For each dataset, a relatively standard set of model covariates were calculated and used. In addition to the Landsat TM channel data (TM bands 1 through 5 and 7), we calculated vegetation indices (NDVI, NIR-corrected NDVI, NDVIc, and NIR-corrected NDVIc), a principal components transformation based on the correlation matrix (retaining the top two components: PCA1 and PCA2), and a tasseled cap transformation (brightness, greenness, and wetness).

Topographic Modeling

Digital elevation models were acquired from the USGS Seamless website (http://seamless.usgs.gov) in March, 2011. These DEMs were mosaicked in ArcGIS, then snapped to the Landsat TM grid and cropped to the study area. Visual inspection of the DEMs demonstrated terrace-like artifacts throughout the mosaic, which would have significantly altered the terrain variables and illumination corrections. Therefore, we applied a weighted smoothing filter that smoothed areas with a high level of terrace artifacts and left areas without artifacts alone (See Appendix A for description of the weighted smoothing filter). From the smoothed DEM, we derived slope, cosine transformed aspect, cosine/slope transformed aspect, sine/slope transformed aspect, topographic roughness index, and compound topographic index. These variables were anticipated to relate to the terrain context of each pixel. For example, cosine transformed aspect is a cosine transformation of the aspect that is centered at south-southwest and relates to the predominance of direct sun during the mid-day and early afternoon. Other topographic variables relate to the hydrological context (e.g.,

compound topographic index is a function of the upslope area and correlates with soil depth, organic matter (Moore et al. 1993)). A full list of both topographic and remote sensing-based variables is given in Table 2.

TRAINING DATA

USDA Forest Service FIA plots were the principle data source used for training data. FIA plots and coordinates were used as ground reference data to generate a dataset of forest structural parameters and predictor variables at each plot location. Plots measured between 2000 and 2010 were imported to the Forest Vegetation Simulator (FVS) Central Rockies growth model variant (Edminster et al. 1991) and projected forward to combine with 2006 and 2010 TM imagery. Therefore, structural parameters for all trees ≥ 1" d.b.h on FIA plots were estimated from sub-models accessed in FVS and projected to 2007 and 2010. Change detection with previous Landsat image dates was used to eliminate forest plots showing disturbance after measurements were taken. Thus, a total of 585 undisturbed FIA plots from both forest and non-forest areas were used to develop predictive models of forest structure using Random Forest regression trees (Breiman 2001).

FOREST STRUCTURE MODELING

The Random Forest regression tree and SP (spatial data) packages in R statistical software (The R Foundation for Statistical Computing 2008) were used to first develop models and implement model runs to produce digital forest structure layers at a 30-m pixel resolution. In general, Random Forest trees use multiple subsets (thousands) of both predictor variables (see Appendix B) and training data (FIA plots) to identify principle relationships in the data. Each model training run is validated using data left out of the bootstrapped sample and errors are aggregated for an overall estimate of model accuracy, a machine learning process known as bootstrapped aggregation or "bagging." Random Forest trees are also capable of estimating variable importance (Breiman 2001). For this research, a tuning algorithm was applied to identify a "best" model using error estimates and variable importance to reduce the number of predictors while attaining similar or higher accuracies as that of a "full" model implemented

with all predictor variables. Multivariate QR matrix decomposition was also used to reduce colinearity among predictor variables (Belsely et al. 1980).

Model validation was implemented using the inverse of the unexplained variance (error) for each predicted forest structure parameter, estimated from data left out of each model iteration (typically one-third of plots). We reserved 25% of the FIA and non-forested point data as an independent validation dataset, leaving them out of the training process altogether.

Forest structure model refinement

Variances explained by all models were used to estimate the best of the six datasets (U, UC, F, FC, M, and MC). Due to the independence of models derived from 2006 and 2010 data, model predictions showed a large variation in predictive error across space, posing critical challenges for quantifying changes in downstream models (e.g., wildlife occupancy models). Therefore, four small-scale focal areas across the study area were identified where the authors had expert knowledge and could qualitatively evaluate model refinements. Basal Area was selected for comparison due to its relatively high accuracy and ease of interpretation. Twenty-four model methods were compared at the four focal areas based on permutations of the; 1) seasonal images used (e.g., both leaf-on and leaf-off vs. leaf-on only), 2) level of linear decorrelation (no QR decomposition and QR decomposition tolerances of 0.05, 0.10, and 0.20), and 3) specific combination of dates the covariates were selected from (e.g., the model year, both years, or 2006 only). Spatial models of basal area were smoothed using a low pass filter to reduce spurious image noise and increase accuracy. Qualitative analysis was used to select the model with the greatest consistency in areas that were known to have not changed significantly between 2006 and 2010.

Results and Discussion

Model and variable performance is shown in Figure 2. In general, the FLAASH+C-corrected and MAD images produced the best models and greater variance explained that models developed with uncorrected imagery. However, models were similar in terms of performance and prediction of forest structure variables. A notable exception was TPA, for

which the U and UC models had the highest (69% variance explained) and lowest (47% variance explained), respectively. TPA was the most difficult variable to predict, with only two models explaining over 50% variance. HGT was the 'easiest' variable to predict, with all models explaining over 80% of the variance. SDI, BA, and CC were also well predicted, with all models explaining over 70% of the variance. QMD was poorly predicted, with only one model (F) explaining over 60% of the variance. Tuned models performed better than untuned models, demonstrating the necessity to use a tuning process to eliminate variables in the modeling process.

Using BA as an example, the most consistent model in no change areas between 2006 and 2010 was the model based on FLAASH-corrected Landsat TM imagery, but overall there were no statistically significant differences in the consistency of the models (Figure 3). Models tended to under-predict at very high BA values, which is a common limitation with Landsat-based predictions of forest structure. No models overpredicted BA above 150 ft^2/ac but M and MC had the most overpredictions in the range of 100 and 150 ft^2/ac BA. Models with illumination correction increased the range of values, suggesting that these models had greater ability to discriminate between areas with otherwise similar spectral characteristics. An example showing the distribution of predicted BA values by the model for uncorrected imagery and FLAASH-corrected/C-corrected imagery is given in Figure 4.

Closer inspection of an area in the North Kaibab Ranger District shows qualitative model differences associated with topography (Figure 5). While both the uncorrected and FLAASH-corrected models have similar predictions no north and south-facing slopes, the IR-MAD and FLAASH-corrected models with a C-correction displayed different predictions. Nevertheless, visual assessments of areas of known disturbance indicated that these models are effective for identifying change over multiple dates (e.g., 2006, 2010; Figure 6).

Although the MAD and FLAASH models performed similarly, we selected FLAASH atmospheric correction for the final models because of the relative ease of implementation as new imagery are analyzed in subsequent years. Therefore, we used FLAASH+C-correction covariates for qualitative model refinement and created 24 model variations based on these layers. The best of the model refinements was judged to be "Leaf on No QR 2yr" model, which

was developed using only terrain variables and satellite imagery from the leaf-on dates (leaf-off was excluded) and a 2-stage process to select covariates. In the first stage, a model combining training data from both leaf-on dates in 2006 and 2010 was developed. In the second stage, separate models from 2006 and 2010 were developed from 2006 and 2010 data, respectively, but model covariates were limited to the covariates from the tuned model in the first stage. The same set of predictor variables showing the best model performance was used for both years.

The "Leaf on No-QR 2yr" model explained less variance than the original FC model (Figure 7) but the original model and BA values were less consistent between dates. Figure 8 shows the differences between 2010 and 2006 predictions for both the original and qualitatively selected models. The standard deviation of the differences between 2010 and 2006 for the qualitatively selected model was 10.2, while the standard deviation for the original model was 19.0. The difference in basal area between 2006 and 2010 from the refined model was also closer to zero for a subset of image pixels (n = 4622) selected across the Kaibab NF on a 1 km x 1 km grid (Figure 8). A greater skewness of BA differences toward negative values was indicative of greater sensitivity to forest change and reduced sensitivity to differences in understory plant phenology (e.g., grasses and forbs). These comparisons showed more consistent BA predictions from the refined model between years, particularly in areas with no apparent disturbance. Use of slightly different seasonal image dates, and variability in understory greenness between years, likely contributed to lower BA consistency in our preliminary models.

The top candidates from the model refinement step were generally based on both years to select covariates (stage 1) and were generally based on the leaf-on dates only. Figure 9 illustrates this step with an example of the five top models for one of our four 'focal' areas on the north rim of the Grand Canyon. Since the goal of the model refinement was to increase consistency across years, these results are not entirely surprising. The selection of covariates from the 2-year model suggests that models based only on the present year may be pick up correlations between predictor variables and image derivatives that are unique to only one year (i.e., because of offset phenology or differential image characteristics such as viewing

geometry); whereas 2-year models are likely identifying covariates that have greater consistency in describing forest characteristics over time. In the latter case, measures of performance may indicate models are better but closer inspection of the predicted spatial distribution of the predicted forest variable reveals greater inconsistency over space. The preponderance of models based on leaf-on dates only is likely due to the low sun angles and increased shading associated with leaf-off dates. Although C-correction aims to correct for variability in illumination due to incidence angle effects, it only works in areas of relatively shallow slopes and does not work in shadowed areas. This study in particular was somewhat limited by the availability of leaf-off dates in 2010 and our selection of 1 November 2010 was not ideal because of the low sun angle. An earlier leaf-off date in October is preferred but in 2006 was not available due to clouds. Given the sensitivity of these models to variations in leaf-off imagery, coupled with the high model performance using leaf-on dates only, we recommend an approach to modeling that utilizes leaf-on dates only.

The most important variables for the original FLAASH-corrected/C-correction models are given in Table 4. Elevation and slope were important in all models and the most important overall. Four of the first five remote sensing variables were all related to greenness during the leaf-off season (NDVIc, NDVI, NDVI4, and greenness). The lone non-greenness variable was band 1, which is most related to albedo. Other top topography-related variables included CTI, a proxy for soil wetness, and cosine-transformed aspect, a proxy for solar exposure.

The most important variables in these final models are indicated in Figure 10. The top variable was elevation, followed by NDVIc and NDVI (all leaf-on dates, since these models only used leaf-on dates). Cosine of aspect and topographic ruggedness index were also very important in most models. Outside of variations of NDVI, reflectance bands did not explain much variation. The best performing reflectance band was band 1, a proxy for albedo. Raw reflectance bands generally did better than principal components bands.

These results highlight the importance of topography and vegetation indices in influencing forest structure. The abundance of leaf-off greenness-related variables highlight the leaf-off period as a time of greater discrimination of forest structural characteristics in the original models. Characteristics of the leaf-off period that may contribute to this result include

the loss of leaves by deciduous trees and the senescence of background understory vegetation. Green understory vegetation may saturate NDVI in areas with incomplete canopy closure and confound results. Models with leaf-off variables had less consistency across years and in all models. It is important to note also that solar angles are problematic during the leaf-off phase and can contribute to problems with overshading, particularly in areas with moderate and steep slopes. Thus, there are trade-offs between models that show good performance and those that produce more consistent forest structure estimates between years. Using images with higher elevation sun angle and more consistent sun illumination improved the ability to monitor forest conditions over time.

A potential source for model differences comes from the modeling approach. Random Forests utilizes a double randomization and thousands of simulations to produce predictive models that predict the greatest amount of variance. Because of the stochastic nature of this approach, similar but different covariates may be selected for model runs (e.g., NDVI vs. NDVIc). This subtle but distinct selection of different predictor variables may result in different predictions, particularly in areas of steep terrain or in areas with high canopy cover where NDVI may become saturated. While we anticipated that illumination correction would boost model predictions on north-facing slopes, the illumination correction itself introduces artifacts on ridgelines due to slight misalignment of DEMs and satellite imagery. For models that rely heavily on illumination-corrected satellite imagery, predictions may be suspect on ridgelines and on steep slopes. Thus, the benefits of illumination correction come with the drawbacks of imprecise topographical effects on terrain shading. Our qualitative analysis of numerous models with varying tuning parameters and methods for selecting covariates suggested that the inclusion of leaf-off date increased model performance for a single image date but decreased consistency across dates. We attribute this to low solar elevation angles associated with the rapidly changing solar elevation during the fall season.

Overall, all models performed similarly with good predictions for HGT, BA, SDI, and CC; moderate predictions for QMD, and poor predictions for TPA. Image normalization via empirical (e.g., IR-MAD normalization) and radiometric (e.g., FLAASH correction) methods improved models over the uncorrected Landsat DNs but the effects of illumination correction are less

clear. Generally, all models had the greatest difficulty with areas of high basal area, which is consistent with other studies of forest structural characteristics using Landsat TM. The inclusion of topographic variables likely increased the predictive power of models but interactions with illumination corrections may have contributed to differences between IR-MAD and FLAASH-corrected models involving illumination correction. Given the qualitative data assessment, we are confident that the FLAASH corrected imagery with c-correction provides the best information regarding forest structural characteristics. With some caution, we suggest that late season leaf-on dates be used as the basis for multispectral covariate determination because solar incidence angles during the leaf-on period are higher and less sensitive to interannual variation in the selection of anniversary dates in image acquisitions. We attribute the lower quality of prediction to areas with high basal area to a combination of pixel saturation common to Landsat TM-based modeling, as well as a dearth of training pixels in areas of high basal area.

MONITORING 'TOOLBOX'

Multi-temporal digital forest structure data layers provide a repeatable and precise means to analyze forest change due to silvicultural treatments in addition to disturbance. To demonstrate data applications, we developed a simple change equation for monitoring the percent forest change for differing forest treatments using data layers as follows:

$$\text{Eq. 1.} \quad \Delta S = (S_2 - S_1/S_1) \times 100,$$

where S_1 is the forest structural variable in time one (2006) and S_2 is the forest structure variable in time two (2010). The absolute value of negative differences multiplied by 100 provides an estimate of percent change. As an example, we used treatment area polygons for management activities completed between 2007 and 2009. These data provide a useful summary of how differing treatment types impact forest density and other conditions important to achieving forest restoration and hazardous fuels mitigation (Figure 6). Contemporary tree thinning and burning approaches produced similar results when compared to group selection silvicultural techniques that remove a greater proportion of basal area (Figure 11).

CONCLUSIONS AND RECOMMENDATIONS

Multiple model iterations were used to establish state-of-the-art image correction and data integration techniques for modeling forest structure and change. FIA plot data, combined with well-calibrated multispectral and multitemporal satellite images, proved capable of producing reliable forest structure estimates over time. The techniques we applied were relatively low-cost, utilizing FIA forest inventory plots and freely available satellite data. Nonetheless, advanced technical skills are needed to apply image and data processing methods to obtain good results.

Based on our comparisons, we recommend that future forest structure data be developed following refined forest structure modeling methods described above. Future image processing should apply atmospheric and terrain correction techniques that improved model outputs and variance explained. Variation in understory vegetation and image characteristics can be controlled by 'matching' image dates (e.g., August or September) between years to control for sun illumination and seasonal effects on model outputs. Models using single image dates produced more reliable forest structure outputs over time. These adjustments showed an enhanced ability to detect area of forest change and no-change, while reducing negative plant phenology impacts on forest structure estimates.

For future modeling efforts, we recommend an approach (e.g., FLAASH-based) that utilizes radiometric principles to convert satellite imagery to surface reflectance before modeling forest structure. The selection of a good leaf-off date is important and should be complemented with an appropriate leaf-on date. Due to increased contrast in shading due to lower solar angles during the leaf-off date, an illumination correction is recommended to correct for topography-induced differences in illumination. Topography data is a critical component of this modeling process and extreme care needs to be taken to ensure quality topographic data is used both in the model and for developing the illumination correction. We outlined a novel technique to eliminate terrace artifacts that manifest in DEM derivatives (e.g., aspect, slope). Good geometrical alignment of the DEM with satellite imagery is also critical because slight misalignment will cause extremely high and low values in illumination-corrections. Given the model performance of IR-MAD vs. FLAASH atmospheric correction, and

given the fact that atmospheric correction has a more rigorous physics-based foundation, we recommend atmospheric correction and illumination correction for future model development. A principle limitation to the strength of these models is the dearth of plots with extremely high values in all predictor variables. The ability to predict areas with high BA, TPA, QMS, SDI, and CC relies on an abundance of training data also with high values. This modeling approach is not effective at predicting beyond the range of the training data and, therefore, it is recommended that additional plots in areas of high BA, CC, and TPA are added for future modeling efforts.

REFERENCES

Belsley, D. A., E. Kuh, and R. E. Welsch. 1980. *Regression Diagnostics*. John Wiley & Sons, Inc., Hoboken, NJ.

Breiman, L., 2001. Random Forests. *Machine Learning* 45:5-32.

Canty, M.J., Nielsen, A.A., Schmidt, M. 2004. Automatic radiometric normalization of multi-temporal satellite imagery. *Remote Sensing of Environment*, 91(3-4):441-451.

Edminster, C.B., Mowrer, H.T., Mathiasen, R.L., Schuler, T.M., Olsen, W. ., Hawksworth, and F.G. 1991. GENGYM: a variable density stand table projection system calibrated for mixed conifer and ponderosa pine stands in the southwest. Res. Paper RM-297. Fort Collins, CO: U. S. Department of Agriculture, Forest Service, Rocky Mountain Forest and Range Experiment Station. 32p.

Moore, I.D., Gessler, P.E., Nielsen, G.A., and Petersen, G.A. 1993. Terrain attributes: estimation methods and scale effects. In Modeling Change in Environmental Systems, edited by A.J. Jakeman , M.B. Beck and M. McAleer (London: Wiley), pp. 189-214.

Song, C., Woodcock, C.E., Seto, K.C., Lenney, M.P., and Macomber, S.A. 2001. Classification and change detection using Landsat TM data: when and how to correct atmospheric effects? *Remote Sensing of Environment* 75:230−244.

Table 1. Acronyms for datasets used in this study. Acronyms reflect the image processing and illumination correction applied to the Landsat TM source imagery.

	Illumination correction	
Normalization technique	None	C-correction
Raw DN (unprocessed Landsat TM)	U	UC
IR-MAD (image-to-image normalization)	M	MC
FLAASH (atmospheric correction)	F	FC

Table 2. List of forest structure covariates used in the modeling and the abbreviations for each used in the rest of this report.

	Forest structure covariates	Abbreviation
Remote sensing variables	Landsat TM1 (leaf-on)	b1_on
	Landsat TM2 (leaf-on)	b2_on
	Landsat TM3 (leaf-on	b3_on
	Landsat TM4 (leaf-on)	b4_on
	Landsat TM5 (leaf-on)	b5_on
	Landsat TM7 (leaf-on)	b7_on
	Landsat TM1 (leaf-off)	b1_off
	Landsat TM2 (leaf-off)	b2_off
	Landsat TM3 (leaf-off)	b3_off
	Landsat TM4 (leaf-off)	b4_off
	Landsat TM5(leaf-off)	b5_off
	Landsat TM7 (leaf-off)	b7_off
	NDVI (leaf-on)	ndvi_on
	NDVI (leaf-off)	ndvi_off
	NDVIc (leaf_on)	ndvic_on
	NDVIc (leaf_off)	ndvic_off
	NDVI/TM4 (leaf-on)	ndvi4_on
	NDVI/TM4 (leaf-off)	ndvi4_off
	NDVIc/TM4 (leaf-on)	ndvic4_on
	NDVIc/TM4 (leaf-off)	ndvic4_off
	NDVI ratio (leaf-on/leaf-off)	NDVI_rat
	NDVIc ratio (leaf-on/leaf-off)	NDVIc_rat
	Brightness (leaf-on)	bright_on
	Greeness (leaf_on)	green_on
	Wetness (leaf_on)	wet_on
	Brightness (leaf-off)	bright_off
	Greeness (leaf_off)	green_off
	Wetness (leaf_off)	wet_off
	TM bands PCA 1 (leaf-on)	pca1_on
	TM bands PCA 2 (leaf-on)	pca2_on
	TM bands PCA1 (leaf-off)	pca1_off
	TM bands PCA2 (leaf-off)	pca2_off
Topography	Elevation	el
	Slope	slope
	Cosine transformed aspect	trasp
	Cos/slope transformed aspect	cos
	Sin/slope transformed aspect	sin
	Topographic ruggedness index	tri
	CTI	cti

Table 3. List of forest structural variables modeled in this study.

Variable	Acronym
Basal Area	BA
Percent Canopy Cover	CC
Forest Height	HGT
Stand Density Index	SDI
Quadratic Mean Diameter	QMD
Trees per Acre	TPA

Table 4. Relative variable importance for FLAASH-corrected, C-corrected models. Variables are ordered by the sum of relative importance over all models. Where relative importance is below 0.01 (1% of the maximum importance), it is denoted by '-'. Variable acronyms are defined in Tables 2 and 3.

Variable	HGT	SDI	BA	CC	TPA	QMD	SUM
el	0.161	0.251	0.331	0.135	0.156	0.186	1.220
slope	0.027	0.099	0.152	0.056	0.121	0.104	0.557
ndvic_off	0.052	0.100	0.179	0.089	-	0.133	0.553
cti	0.027	0.099	-	0.044	0.163	0.093	0.426
cos	0.032	0.089	-	0.048	0.140	0.114	0.424
ndvi_off	0.030	0.101	0.115	0.058	-	0.091	0.395
b1_on	0.027	0.107	0.124	0.049	-	-	0.307
ndvi4_off	0.021	0.064	0.100	0.047	-	0.069	0.301
green_off	0.029	-	-	0.053	0.115	0.089	0.286
ndvi_on	0.030	-	-	0.041	0.158	-	0.230
b4_off	0.023	-	-	0.034	0.146	-	0.203
green_on	0.022	-	-	0.031	-	0.121	0.174
tri	0.038	0.092	-	0.041	-	-	0.171
b7_on	0.030	-	-	0.041	-	-	0.071
ndvi_rat	0.028	-	-	0.039	-	-	0.067
pc3_off	0.023	-	-	0.037	-	-	0.061
sin	0.018	-	-	0.041	-	-	0.059
b5_off	0.026	-	-	0.033	-	-	0.059
b3_on	0.020	-	-	0.032	-	-	0.052
pc2_on	0.016	-	-	0.029	-	-	0.045
b2_on	0.020	-	-	0.021	-	-	0.041
b7_off	0.033	-	-	-	-	-	0.033
ndvic_on	0.028	-	-	-	-	-	0.028
wet_on	0.028	-	-	-	-	-	0.028
ndvi4_on	0.027	-	-	-	-	-	0.027
wet_off	0.024	-	-	-	-	-	0.024
b3_off	0.024	-	-	-	-	-	0.024
pc1_on	0.021	-	-	-	-	-	0.021
bright_off	0.021	-	-	-	-	-	0.021
pc2_off	0.020	-	-	-	-	-	0.020
b4_on	0.020	-	-	-	-	-	0.020
b1_off	0.020	-	-	-	-	-	0.020
trasp	0.019	-	-	-	-	-	0.019
b2_off	0.016	-	-	-	-	-	0.016

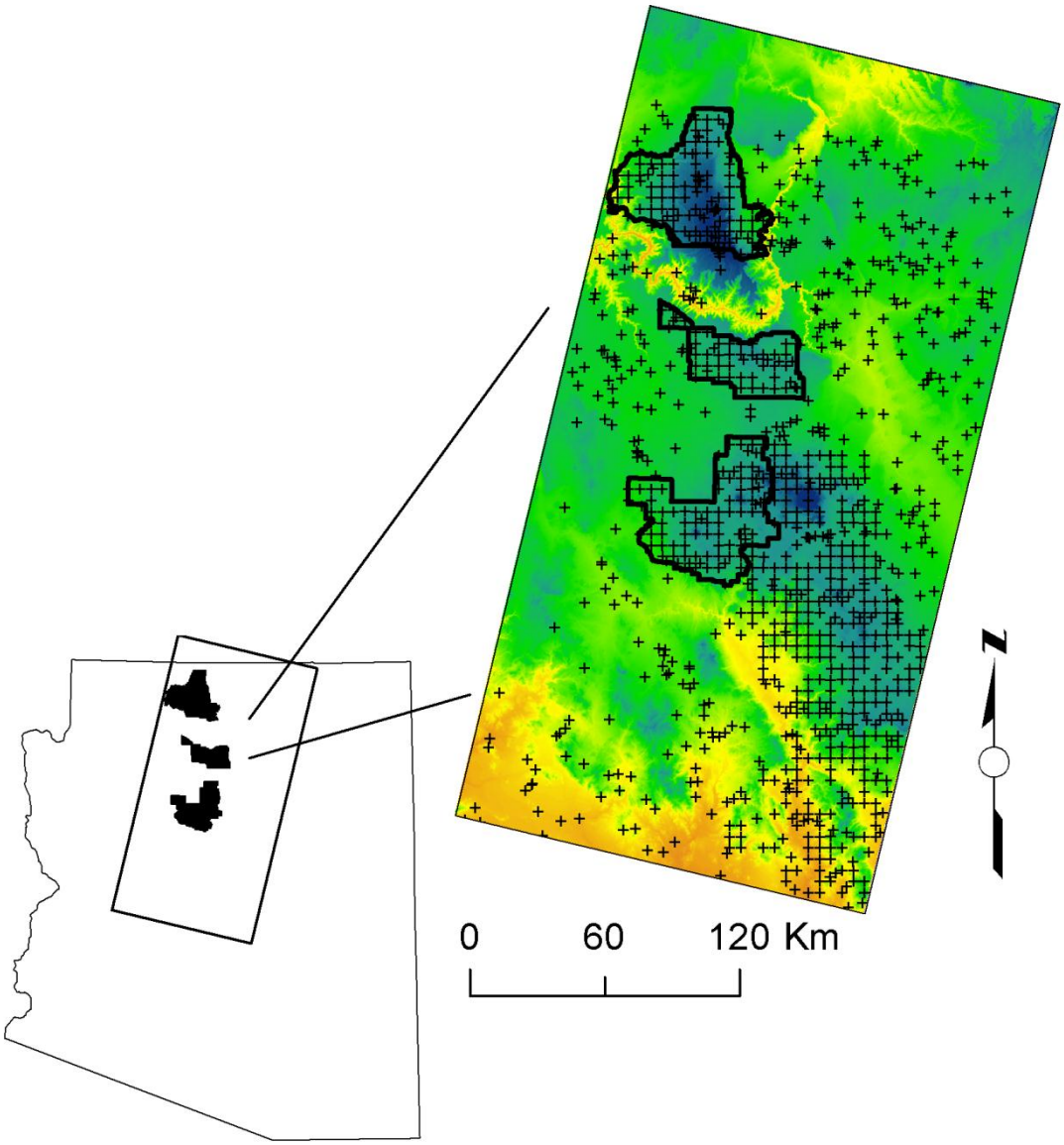

Figure 1. Map showing study area with respect to Kaibab National Forest boundaries (solid bold line) and training plots. Training plots include systematically located FIA plots and non-forested points.

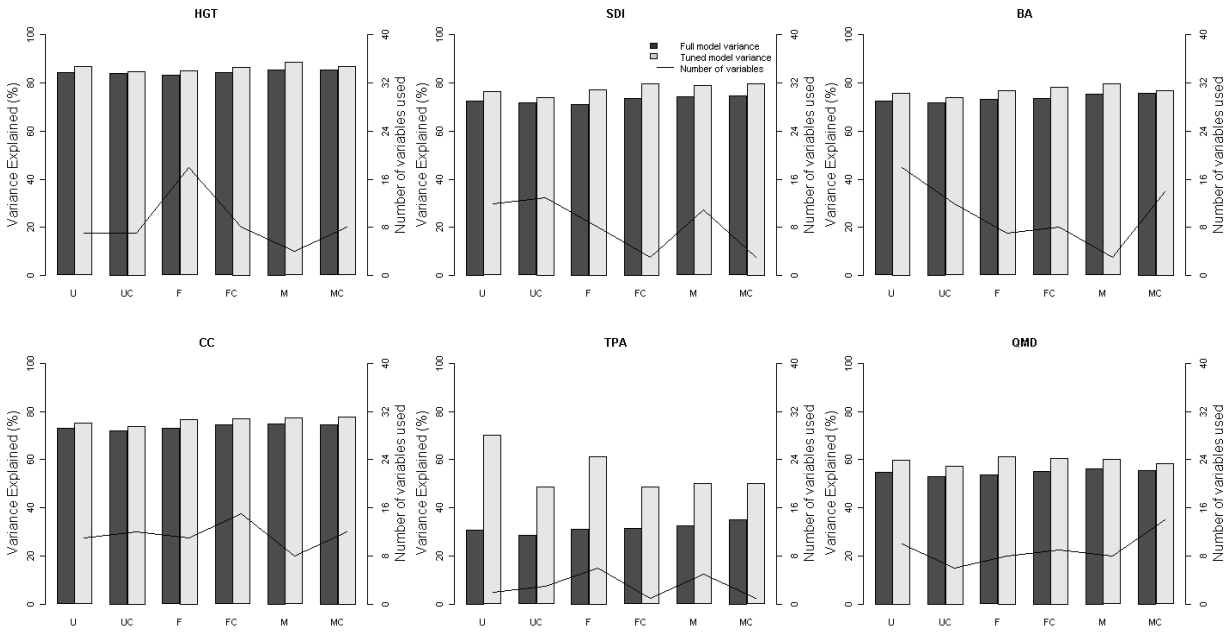

Figure 2. Variance explained and number of variables used in six forest structural variables for six different image treatments (x-axis; U, UC, F, FC, M, and MC). Untuned and tuned models are shown. Variable acronyms are defined in Table 3.

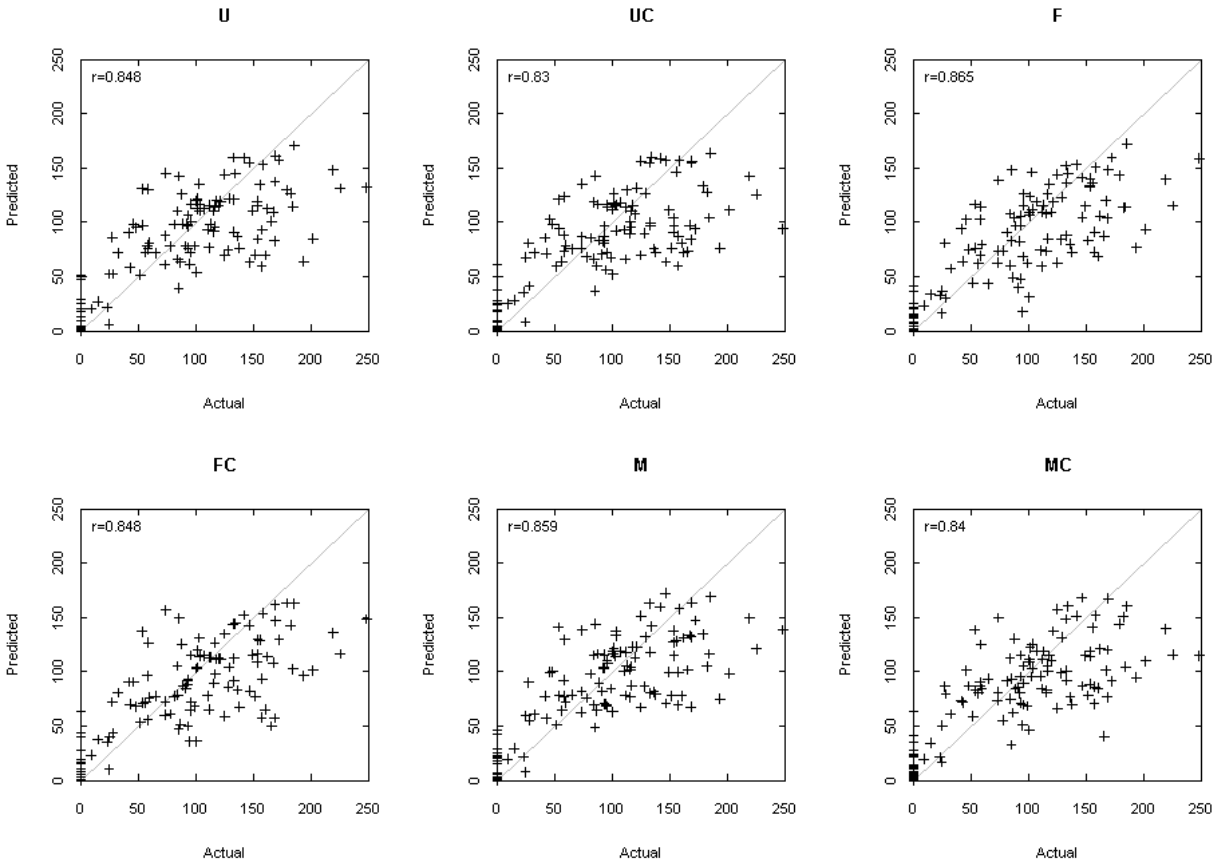

Figure 3. Scatter plots of actual vs. predicted basal area for the validation data withheld from modeling for the six different classes of image treatments. Pearson's r correlation for each model is inset into each plot. Although not significantly different, the FLAASH and MAD corrections had the best predictions on the validation data. In general, all models tended to underpredict basal area at higher basal area values.

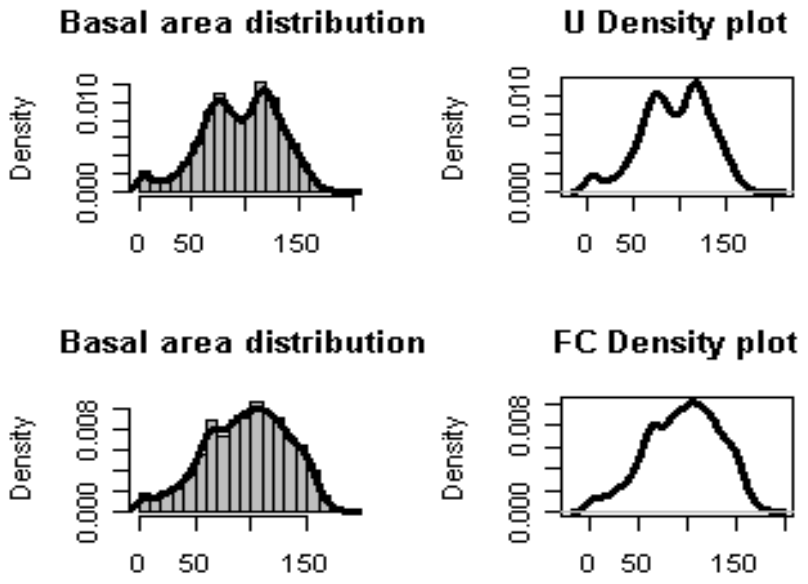

Figure 4. Basal area (BA; ft^2/ac) density plots for 2006 A) uncorrected (U) and B) FLAASH/C-corrected (FC) TM imagery from an array of 1km x 1km points (*n* = 4622) overlapping the Kaibab National Forest. Forest structure variables modeled from uncorrected imagery were sensitive to terrain effects, as noted by an uneven BA distribution and lower density near 100 ft^2/ac.

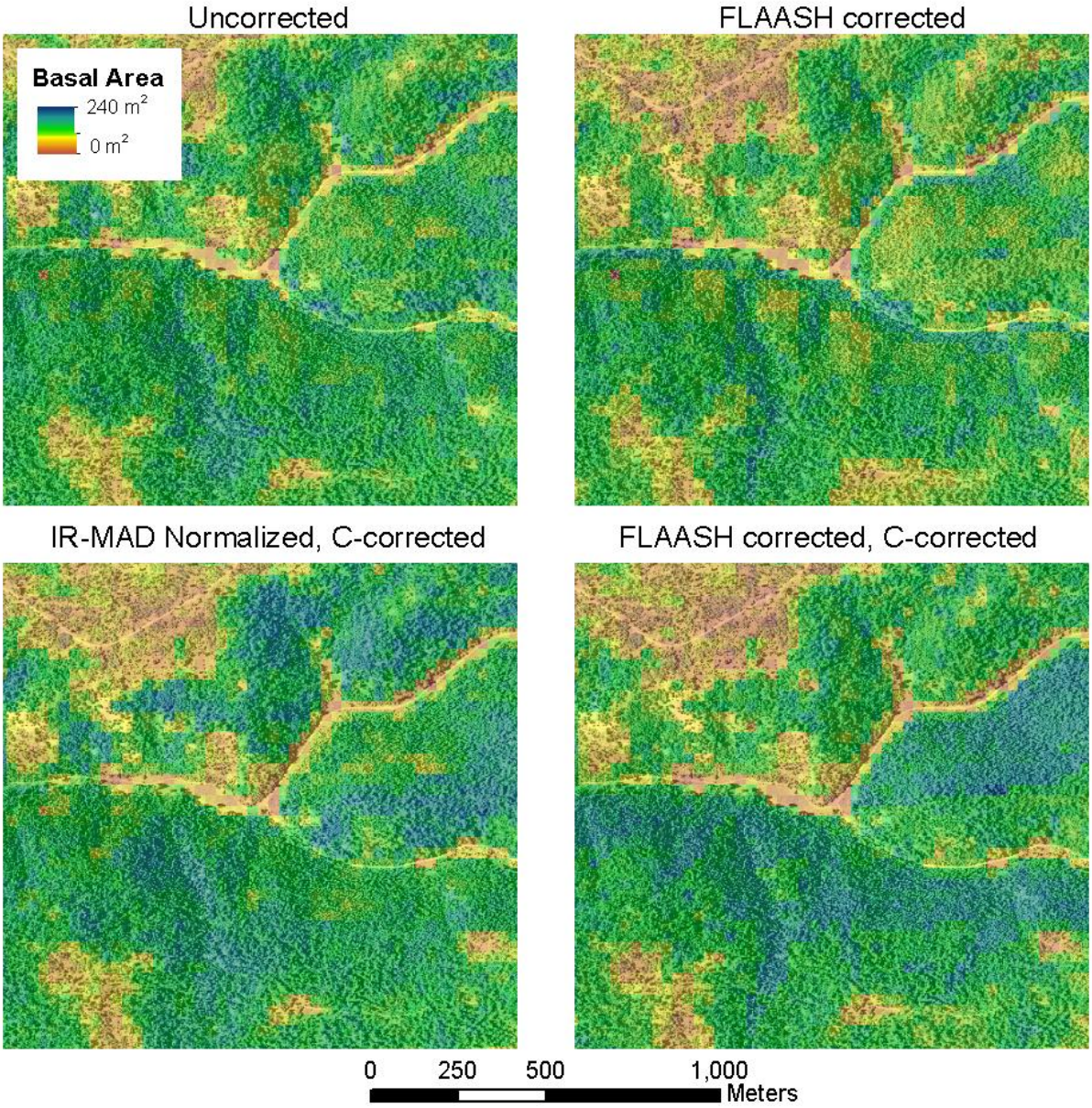

Figure 5. Detail of four different model predictions on the North Kaibab Ranger District. The panels represent the uncorrected model, the FLAASH-corrected model, the IR-MAD+C-correction, and the FLAASH-corrected, C-correction models. Of particular interest is the role of topography (north- vs. south-facing slopes) when comparing the four models. While uncorrected and FLAASH-corrected images are relatively similar, the IR-MAD and FLAASH-corrected with illumination correction have different behavior on north vs. south-facing slopes. More specifically, the IR-MAD model predicted greater basal area on south-facing slopes while the FLAASH corrected image predicted greater basal area on the north-facing slopes.

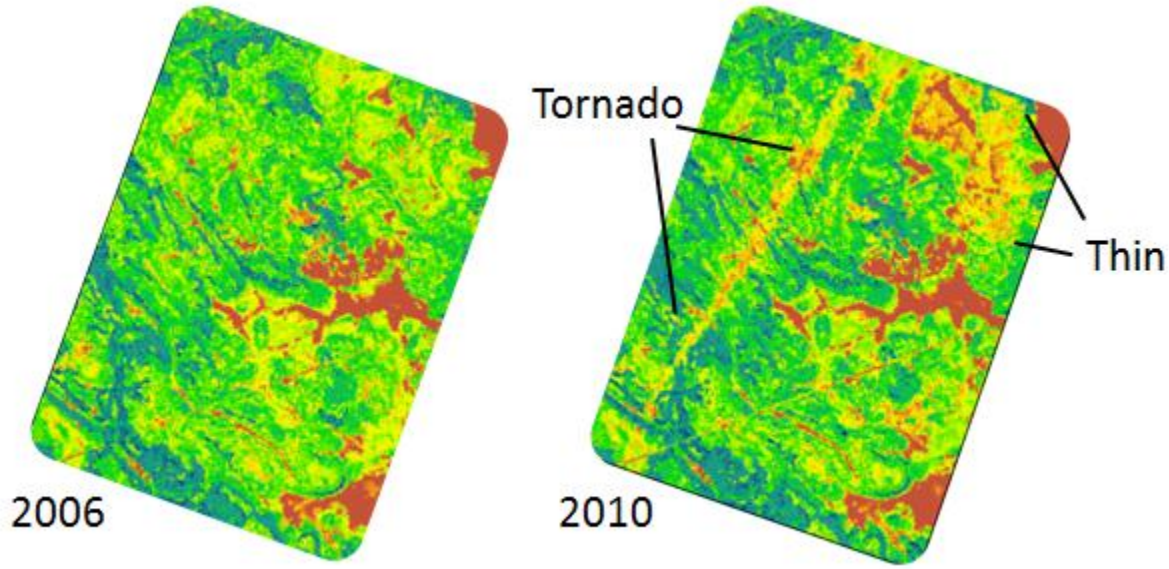

Figure 6. Example of changes in basal area between 2006 and 2010 predicted by the FLAASH-based, C-corrected model. The path of the major tornado from the tornado events of 2010 is clearly shown in the 2010 model, as is a large area of thinning treatments.

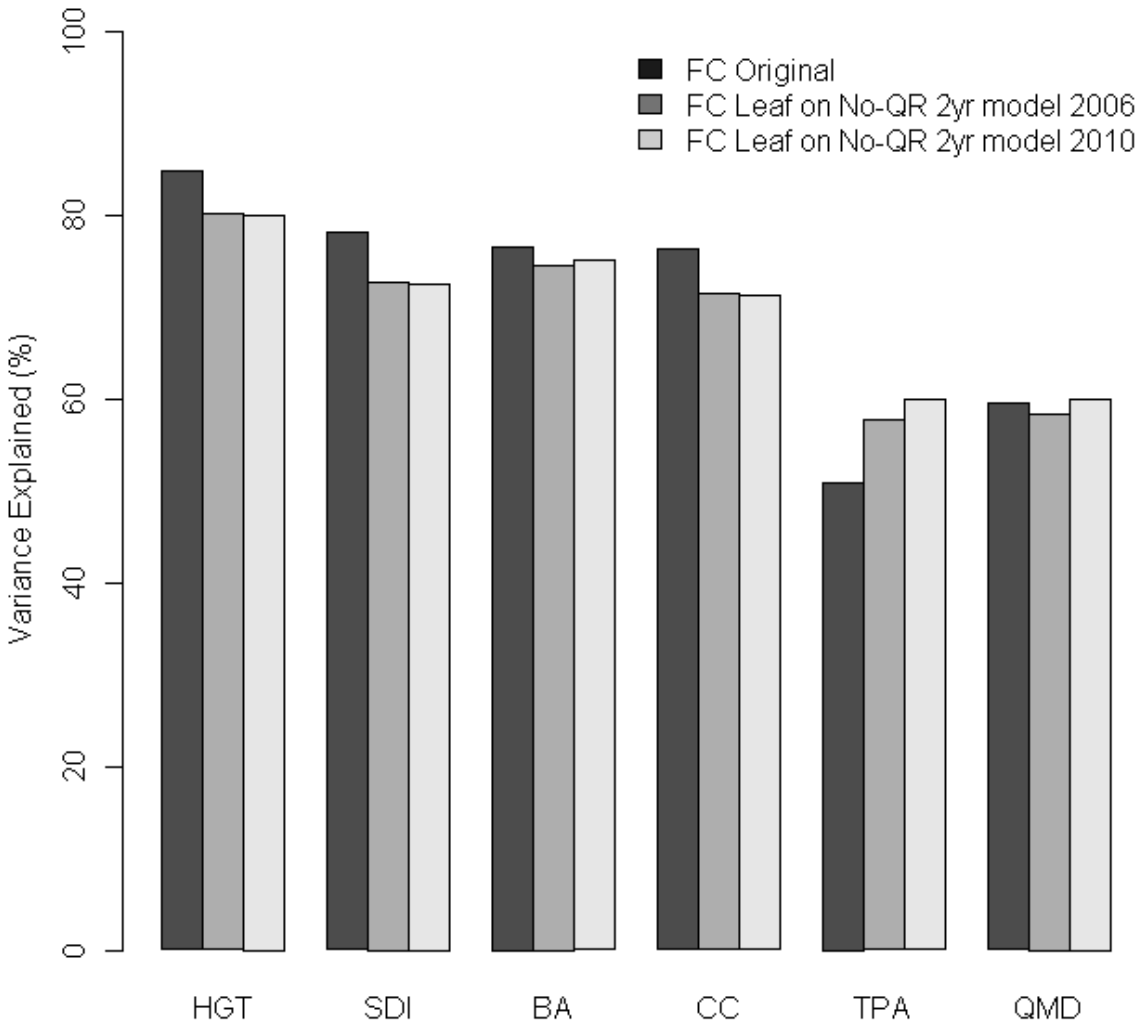

Figure 7. Variance explained by FC original (repeated from Figure 2) in relation to the best model from a qualitative standpoint ("Leaf on No-QR 2yr") from 2006 and 2010. For six forest structure variables. Variable acronyms are defined in Table 3. Although the original FC models performed better than the "Leaf on No-QR 2yr" models, they were more consistent from 2006 to 2010 which results in greater confidence in estimating interannual change and is better for downstream models such as occupancy models which rely on these data.

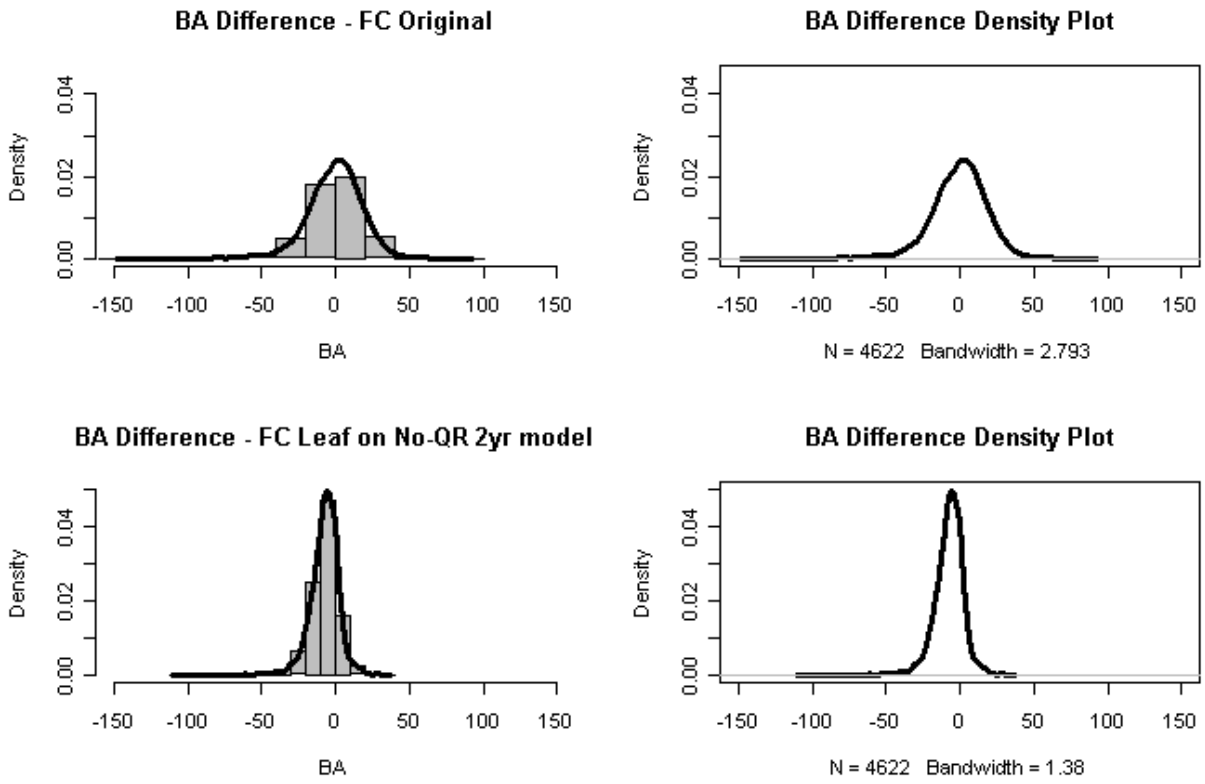

Figure 8. Density plots of Basal Area from the original FLAASH+C-corrected imagery (top row), the FC Leaf on No-QR 2yr model indicating improved consistency for refined basal area model (bottom row).

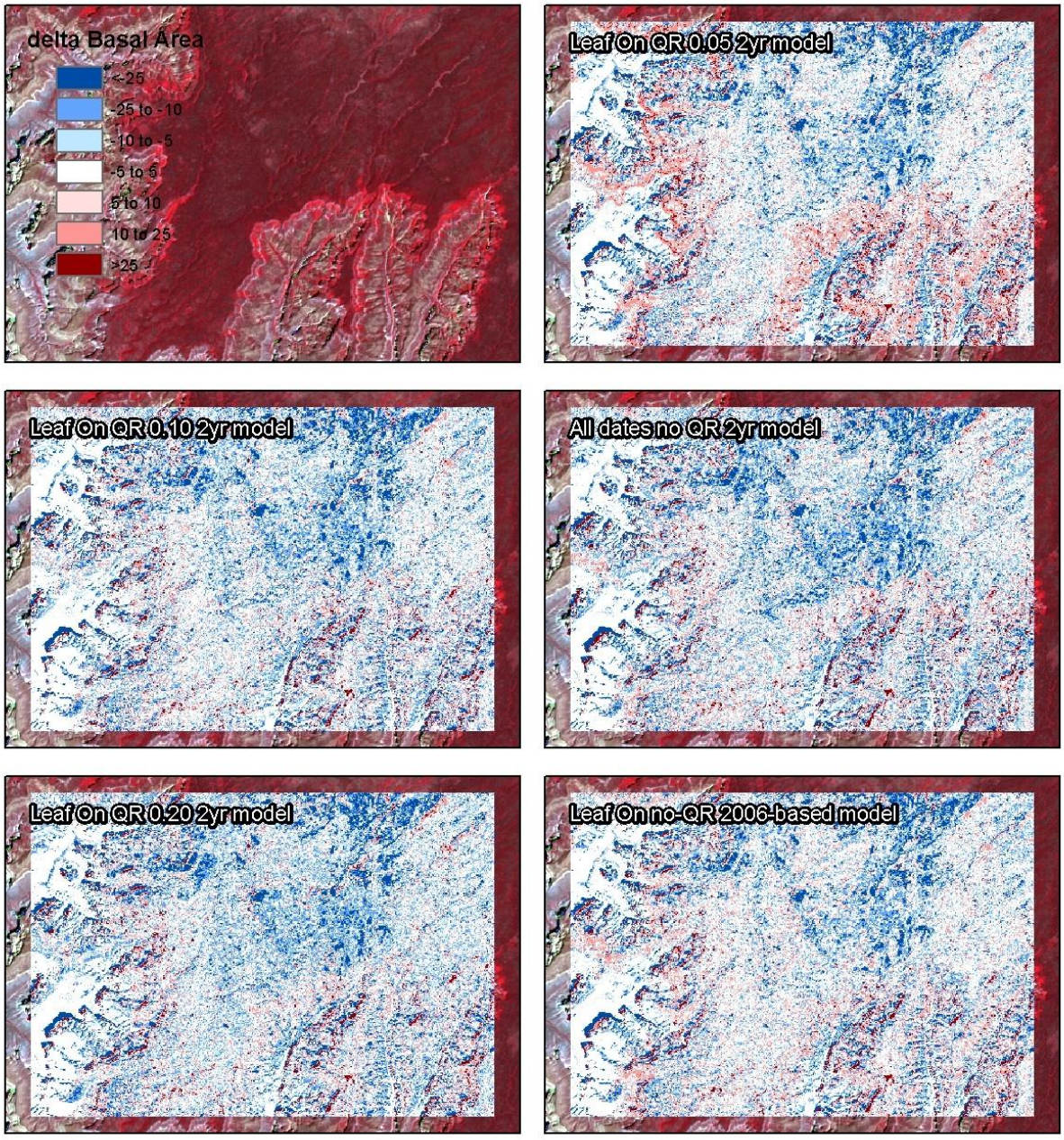

Figure 9. Difference in Basal Area (BA) between 2010 and 2006 as predicted by five models at the north rim of the Grand Canyon. Areas in blue and red have the greatest differences in predicted BA between the two years whereas areas in white or light colors are predicted to have little or no change. These five models were judged to be the best of the 24 refined models because of the prevalence of no change areas. As an example, the "Leaf on QR 0.05 2yr model" (upper right) shows the greatest change bias as indicated by the contiguous red areas on the canyon slopes and was considered to be the worst of these five models.

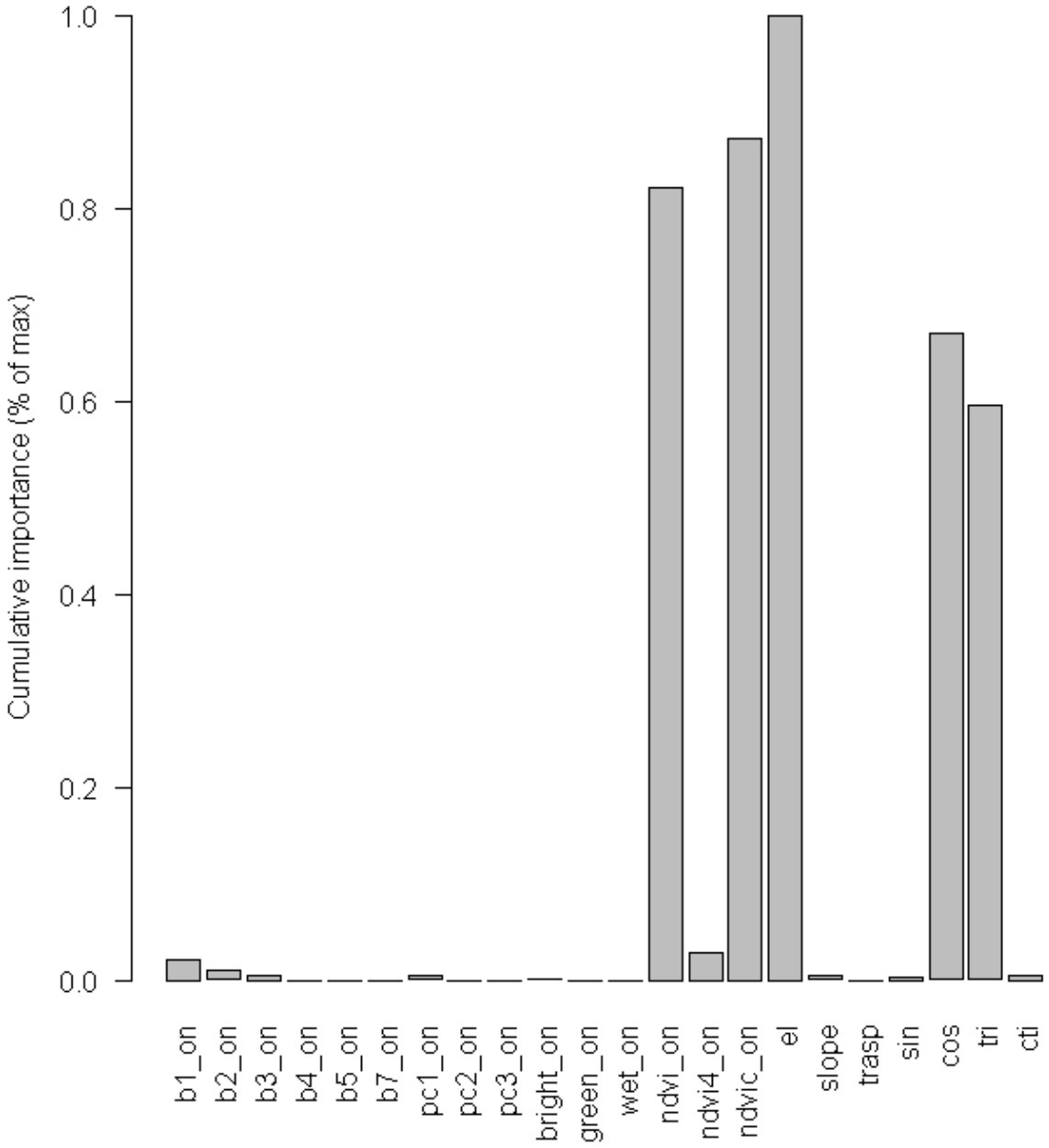

Figure 10. Cumulative variable importance for final FLAASH-corrected/C-correction models. Variable importance was summed over all models and divided by the elevation (el)that explained the greatest combined variance.

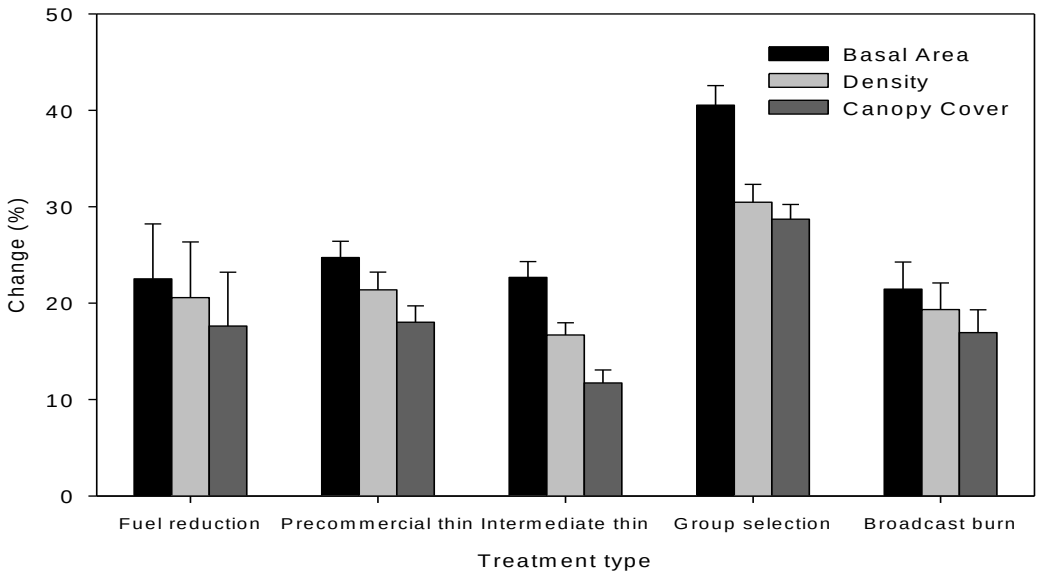

Figure 11. Percent change in forest structure variables for estimating the impact of common treatment types, such as small diameter tree thinning techniques, group selection, and broadcast burning implemented on the Kaibab National Forest between 2007 and 2009.

Appendix A. Weighted DEM Smoothing

A 30-m NED Digital elevation model (DEM) was obtained from the USGS Seamless website on May 15, 2011, as a number of overlapping tiles, then mosaicked and clipped to the study area. Inspection of derivative products such as slope and aspect indicated terrace artifacts were abundant in some regions of low relief so we applied a weighted smoothing to combine a smoothed surface with the original DEM in order to minimize the artifacts. The weighted smoothed DEM was calculated as:

$$DEM_{wt.sm} = (1 - w) * DEM + w * DEM_{sm},$$

where DEM_{sm} represents the original DEM smoothed using a low-pass circular filter with radius of 7 pixels and w represents the neighborhood-level estimation of contour artifacts in the range of [0,1]. The calculation of w is based on an algorithm with four steps:

1) Create a binary mask of all cells with slope values of 0.
2) Grow the mask by 3 cells.
3) Modify the mask based on a majority filter over circular neighborhood with radius of 3 pixels.
4) Blur the mask by applying a low pass filter to a circular neighborhood with radius 7.

Step 4) provides a spatial representation of w. A comparison of DEM, DEM_{sm}, $DEM_{wt.sm}$, and w are provided in Figure A1. In the figure, the undesirable artifacts and desirable high-resolution relief from DEM are visible in DEM and missing in DEM_{sm}, whereas in $DEM_{wt.sm}$, it is apparent that the undesirable artifacts have been eliminated and high-resolution relief has been preserved.

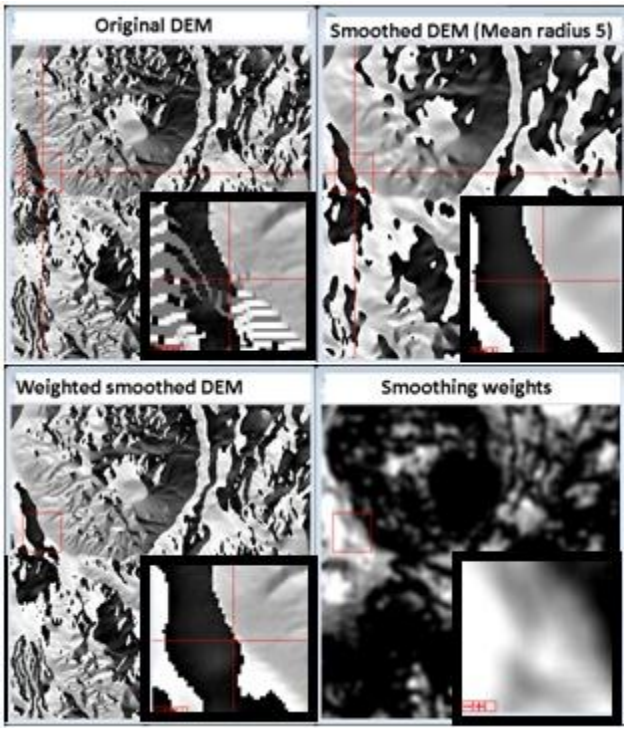

Figure A1. Examples of Original DEM, Smoothed DEM, Weighted Smoothed DEM, and smoothing weights. Each panel shows a landscape-scale map of a DEM hillshade with an inset view. Terraces are seen clearly in the inset view. The terraces have been eliminated in the smoothed DEM but so has the shallow drainage in the northeast of the inset map. The weighted smoothed DEM shows both the smoothed terraces and the drainage feature. The smoothing weights are shown for the mapped area to indicate the extent of terraces detected (in white).

Appendix B. Detailed descriptions of all covariates used in the models.

LANDSAT TM1-5,7

Landsat TM1-TM5 and TM7 are the 6 reflective channels for Landsat TM and represent the upwelling radiance in the blue (0.45-0.52 µm), green (0.52-0.60 µm), red (0.63-0.69 µm), near-infrared (0.76-0.90 µm), and shortwave infrared (1.55-1.75 and 2.08-2.35 µm).

NDVI

Normalized Difference Vegetation Index, or NDVI, is the normalized difference between the near-infrared (NIR) and red reflectance and is defined by the formula:

$$NDVI = \frac{NIR - Red}{NIR + Red}$$

NDVI is correlated with vegetative cover because chlorophyll absorbs strongly in the red spectrum and cell walls reflect in the near-infrared spectrum.

Tucker, C. J. (1979) Red and photographic infrared linear combinations for monitoring vegetation. Remote Sensing of Environment, 8:127-150.

$NDVI_c$

$NDVI_c$ is a modification to NDVI specifically for conifer forest and relies on shortwave-infrared to account for canopy closure:

$$NDVI_c = \frac{NIR - Red}{NIR + Red}\left(1 - \frac{SWIR - SWIR_{min}}{SWIR_{max} - SWIR_{min}}\right)$$

where $SWIR_{min}$ and $SWIR_{max}$ are the minimum and maximum shortwave-infrared reflectance in areas with completely open and completely closed canopies, respectively (Nemani et al. 1993).

Nemani, R.; Pierce, L.; Running, S. 1993. Forest ecosystem process at the watershed scale: Sensitivity to remotely-sensed leaf area index estimates. *International Journal of Remote Sensing*, 14: 2519–2539.

NDVI/TM4

NDVI is somewhat sensitive to low NIR values. Dividing by NIR increases contrast for low values of NIR:

$$NDVI = \frac{NIR - Red}{(NIR + Red) \times NIR}$$

NDVI ratio (leaf-on/leaf-off)

This is a two-date variable that utilizes NDVI from the leaf-on and leaf-off date. This should discriminate between deciduous and evergreen areas because deciduous forests have high NDVI during leaf-on and low NDVI during leaf-off periods

Brightness, Greenness, and Wetness (Tasseled Cap)

The Tasseled Cap transformation is a specific transformation that recombines the channel data from Landsat TM into a smaller set of unrelated variables. It was developed as a principal components analysis (PCA) but it was observed that PCA tended to produce similar outputs on most scenes. Therefore, the Tasseled Cap was developed as a standard transformation of Landsat data. The first three components of the Tasseled Cap transformation are related to brightness (albedo), greenness, and wetness.

TM bands PCA

Principal Components Analysis (PCA) is a process in which Landsat TM data is recombined to form a new set of bands that are each a weighted sum of band values. PCA creates an orthogonal transformation of the input data such that each PC output band is linearly independent from other PC bands. PC bands are ordered such that the first PC describes the greatest amount of variance, followed by the second, third, and so on. For this study, we used the first and second PC bands.

Elevation

Elevation is the vertical distance in meters at a pixel, derived from a digital elevation model (DEM).

Slope

Slope is the percentage of maximum change in elevation at a pixel.

Cosine transformed aspect

Aspect is continuous from 0 to 360 degrees but discontinuous from 360 to 1 degrees. Cosine transformation of aspect transforms aspect into a measure of 'northness' and 'southness.' Thus, negative values are associated with south-facing slopes and positive values are associated with north-facing slopes.

Cos/slope transformed aspect

Like the cosine transformed aspect, the cos/slope transformed aspect translates aspect onto the scale of -1 (south) and 1 (north) but modifies it by the slope such that areas of higher slope have more extreme (positive or negative) values.

SIN/SLOPE TRANSFORMED ASPECT

Cos/slope transformed aspect translates aspect onto the scale of -1 (west) and 1 (east) but modifies it by the slope such that areas of higher slope have more extreme (positive or negative) values.

TOPOGRAPHIC RUGGEDNESS INDEX

Topographic Ruggedness Index (TPI) is a measurement expressing the elevation difference between adjacent cells in a DEM.

Riley, S. J., S. D. DeGloria, and R. Elliot (1999). A terrain ruggedness index that quantifies topographic heterogeneity, Intermountain Journal of Sciences, vol. 5, No. 1-4,1999.

COMPOUND TOPOGRAPHIC INDEX

Compound Topographic Index (CTI) is a steady state wetness index that is a function of the slope and upstream contributing area. Jeff Evans describes the variable on the ESRI arcscripts forum (http://arcscripts.esri.com/details.asp?dbid=11863):

> *CTI is a steady state wetness index. The CTI is a function of both the slope and the upstream contributing area per unit width orthogonal to the flow direction. CTI was designed for hillslope catenas. Accumulation numbers in flat areas will be very large and CTI will not be a relevant variable. CTI is highly correlated with several soil attributes such as horizon depth(r=0.55), silt percentage(r=0.61), organic matter content(r=0.57), and phosphorus(r=0.53) (Moore et al. 1993).*
>
> *The implementation of CTI can be shown as:*
> *CTI = ln (As / (tan(beta)) where As = Area Value calculated as (flow accumulation + 1) *(pixel area m2) and beta is the slope expressed in*
> *radians.*
>
> *References:*
>
> *Gessler, P.E., I.D. Moore, N.J. McKenzie, and P.J. Ryan. 1995. Soil-landscape modeling and spatial prediction of soil attributes. International Journal of GIS. Vol 9, No 4, 421-432.*
>
> *Moore, I D., Gessler, P.E., Nielsen, G.A., and Petersen, G.A. 1993. Terrain attributes: estimation methods and scale effects. In Modeling Change in Environmental Systems, edited by A.J. Jakeman, M.B. Beck and M. McAleer (London: Wiley), pp. 189 - 214.*

Spatially Explicit Estimates of Occupancy Probability for Three Songbird Species on the Kaibab National Forest

BACKGROUND AND JUSTIFICATION

Songbirds are considered to be responsive to a variety of "environmental quality" attributes, and are commonly monitored to assess the impacts of management activity due to their sensitivity to changes in vegetation structure and composition (Saracco et al. 2008; Dickson et al. 2009). Additionally, species designated by the U.S. Forest Service as Management Indicator Species (MIS) are those whose population changes are believed to "indicate the effects of management activities" (Stein Foster et al. 2010). Population changes are usually assessed by estimating how density or abundance changed over time or in response to management actions. A variety of techniques have been developed to reduce bias in density and abundance estimates that results when species are detected imperfectly or infrequently, as is often the case with songbirds (Rosenstock et al. 2002; Dickson et al. 2009). Many of these techniques, however, require moderate-to-large sample sizes to generate estimates with the necessary precision to detect trends or environmental (e.g., habitat) relationships (MacKenzie et al. 2005).

Occupancy, in cases where sample sizes are large, can be defined as the proportion of total area occupied and can provide a useful alternative to density or abundance, especially for uncommon species (MacKenzie et al. 2006). More generally, occupancy also can be interpreted as the probability of locating an individual of species *x* in location *y*. This interpretation (probability of occupancy) reflects an a priori expectation that a site will be occupied based on a hypothesis about the underlying process determining occupancy. The former interpretation (proportion of area occupied) is the realization of that process, given large sample sizes (MacKenzie et al. 2006). Recent advances in occupancy estimation techniques allow habitat covariates to be incorporated into estimates of occupancy, colonization, and local extinction while accounting for detection probability resulting in estimates that are less biased than naïve estimates (i.e., those that assume perfect detectability) (MacKenzie et al. 2003; MacKenzie et al. 2006).

Site occupancy can be used in a monitoring context to reflect the current state of the population and, through multi-season extensions, provide information on population trends. Estimating occupancy often requires fewer detections than other density estimation techniques allowing for more precise estimates of rare or infrequently detected species (MacKenzie et al. 2003; MacKenzie et al. 2005). Furthermore, efforts to relate occupancy to habitat or environmental covariates allow estimation and prediction of changes in population state due to coarser-scale changes in land-use and climate (e.g., Dickson et al. 2009; Mattsson & Marshall 2009). Deriving these habitat-occupancy relationships using high-resolution satellite imagery provides the opportunity to identify the impacts of more localized changes (e.g., forest restoration treatments) across larger spatial scales.

The Kaibab National Forest (KNF) recently began a formal Land Management Plan revision process (NFMA 1976). Establishing current trends for MIS (Stein Foster et al. 2010), identifying potential new MIS, and developing monitoring strategies to assess management impacts on those species are integral components of the plan revision process. Here, we leveraged data collected through the KNFs songbird monitoring program to derive baseline estimates of occupancy and identify environmental variables likely to be impacted by future forest management that influence occupancy. For three species of songbird, we used multi-season data and multi-model inference to develop models that predict occupancy dynamics (e.g., probabilities of detection, occupancy, colonization and local extinction), provide new information on temporal trends in occupancy, and generate spatially explicit, probabilistic surfaces within a GIS that permit the identification of areas with relatively high and low occupancy under current conditions. In addition, these models can be used in conjunction with a suite of tools designed to rapidly derive forest structural attributes from subsequent Landsat TM imagery (see above section) to identify changes in occupancy due to forest management activities. The following report describes the results for three proposed MIS (Grace's Warbler (*Dendroica graciae*), Ruby-crowned Kinglet (*Regulus calendula*), and Western Bluebird (*Sialia mexicana*)) known to occupy mixed-conifer, ponderosa pine, and piñon-juniper dominated areas.

METHODS

AVIAN SURVEYS

The KNF initiated point-transect songbird surveys in 2005. Thirty-five transect lines were randomly assigned within aspen, montane grassland, ponderosa pine, mixed-conifer, and piñon-juniper vegetation types based on stand exam data. Additional transect lines were established using the same assignment protocol in 2006, 2007, and 2008 for a total of 90 transects within the ponderosa pine, mixed-conifer, and piñon-juniper vegetation types. The aspen and montane grassland vegetation types were eliminated from sampling after the 2006 season (B. Noble, 2010 USDA Forest Service Four Forest Restoration Initiative Core Team, personal communication). USFS personnel conducted 5-minute point counts at locations along each transect line in 2005 and 2006 using a 100-m fixed radius distance sampling protocol (Buckland et al. 2001). The Rocky Mountain Bird Observatory was contracted to conduct all surveys in subsequent years using 125-m fixed radius distance sampling and their standard habitat-stratified point-transect protocol (Hanni et al. 2009).

DERIVATION OF ENVIRONMENTAL VARIABLES

Within a GIS (Geographic Information System; ArcGIS v9.3.1, Environmental Systems Research Institute, Inc., Redlands, CA), we spatially defined linear transect locations using the global positioning system (GPS) coordinates of individual points along each transect line. We then buffered each transect by 125 m and computed multiple statistics (e.g., mean, standard deviation, majority, variety) for the environmental variables below within this buffered extent using zonal statistics.

We derived management-relevant forest structural variables predicted to influence patterns of songbird occupancy using data from spatially referenced USDA Forest Service Forest Inventory and Analysis (FIA) plots and terrain corrected and radiometrically calibrated multi-date Landsat Thematic Mapper imagery (30-m pixel resolution). Methods for producing these

structural variables are described in detail in the previous section. Within the GIS, we used 30-m resolution data obtained from the interagency LANDFIRE (Landscape Fire and Resource Management Planning Tools) program website (www.landfire.gov), including derivatives of the National Elevation Dataset (NED; slope and aspect), to model additional environmental and terrain features. Expected vegetation type (EVT) and variation in EVT were derived using the latest 'rapid refresh' version of LANDFIRE EVT data and calculated using a majority and variety estimate within each buffered transect. As a surrogate for unmeasured mesic conditions, we estimated the degree of northeastern orientation of each transect using the sum of all cosine transformed values of aspect within a buffered transect (result scaled between 0.0 and 1.0).

Each of the above environmental variables was derived at a 30-m resolution prior to analysis. Prior to implementing our occupancy models, we standardized and rescaled values for all continuous environmental variables to a mean of zero and unit variance (Neter et al. 1996). We also calculated correlations between values of all pairs of environmental variables among all survey transects. Some variables, including tree density, had univariate correlation coefficients > 0.70 and were therefore excluded from our analyses; all other pairs of variables were not highly correlated and were considered in our analyses.

Single Season Models of Occupancy

We used the single season occupancy framework of MacKenzie et al. (2006) to estimate probabilities of occupancy and detection for the period 2006–2009. Data from 2005 were not used due to insufficient sample size for estimating detection probability. We defined occupancy (ψ) as the expected probability that a given site (i.e., transect) was occupied by a species during the period of analysis and detection probability (p) as the probability of detecting the species at a site if it was present during a count in that period (Dickson et al. 2009; MacKenzie et al. 2006). We derived estimates for each parameter separately based on "full" models that simultaneously included the most parsimonious model for the other parameters (Dickson et al. 2009). We used Akaike's Information Criterion (AIC; Burnham & Anderson 2002) to identify the "best" model(s) among a candidate set of nested models that each represented *a priori*-determined combinations of the environmental covariates defined above (Table 1). We also included null models of occupancy and detection probability (denoted

by 'dot' models) within each candidate set to evaluate the performance and fit of the "best" models (Anderson 2008). We considered candidate models with AIC difference (ΔAIC) values < 4.0 as those that best approximated the data and used these models to calculate model-averaged regression coefficients and unconditional standard errors (Burnham & Anderson 2002). Strong predictors were evaluated by dividing regression coefficients by their unconditional standard error to calculate the *Z*-statistic for each variable. A predictor with a *Z* value >|2.0| was determined to be a reasonably strong predictors of occupancy, with the sign of the *Z* value used for interpretation of the nature of the relationship (Dickson et al. 2009). Models that failed to converge or produced invalid parameter estimates were not considered in model sets used for inference. We conducted all analyses using the single season occupancy estimation routine in program PRESENCE (v2.2; Hines 2006).

Spatially Explicit Models of Occupancy

For each species, we used model-averaged estimates of the regression coefficients obtained with the single season routine in PRESENCE to build a continuous response surface within the GIS based on forest structural attributes in 2006 and then again in 2010. This spatially explicit model predicted (i.e., estimated) the relative probability of occupancy across the study area at a 30-m resolution for both time periods.

Dynamic Models of Occupancy

We utilized the multi-season occupancy modeling framework of MacKenzie et al. (2003, 2006) and Dickson et al. (2009) to estimate probabilities of detection, occupancy, colonization (γ), and local extinction (ε) for 2006-2009. Following MacKenzie et al. (2006), colonization was defined as the probability that an unoccupied site in a given season was occupied by a species the following season and local extinction as the probability that a site occupied by a species in a given season was unoccupied the following season. We assumed that annual changes in colonization and local extinction represented dispersal and temporary emigration, respectively. Again, 2005 was not included in our analysis due to insufficient sample size. In order to illustrate trends in occupancy, we derived initial estimates of occupancy for 2006 and then estimated subsequent, year-specific estimates for 2007-2009 by modeling probabilities of

colonization and local extinction (MacKenzie et al. 2003). We conducted all analyses using the multi-season occupancy estimation feature in program PRESENCE.

RESULTS

AVIAN SURVEYS

A total of 3427 surveys were conducted from 2006–2009, with the greatest number of counts (*n* = 1183) conducted in 2008 and the fewest (387) in 2006. Grace's Warbler and Ruby-crowned Kinglet had more detections in 2009 than any other year (255 and 241 detections, respectively), while Western Bluebird were detected more frequently in 2008 (186 detections). Grace's Warbler, Ruby-crowned Kinglet, and Western Bluebird were detected a total of 764, 695, and 483 times, respectively, across all years of the study. With the exception of a marked decrease for Ruby-crowned Kinglet between 2005 and 2006, detection probabilities were not highly variable, but generally much less than 1 (i.e., < 0.50; Figure 1).

SINGLE SEASON MODELS OF OCCUPANCY

For each species, models relating environmental variables to probability of occupancy performed better than the null model ($\Delta AIC<12.4$; AIC model weight 0.26 – 0.47); however, results for Grace's Warbler and Ruby-crowned Kinglet indicated a much stronger relationship with environmental variables while a more intermediate relationship was seen for Western Bluebird (Table 1). Basal area and canopy cover were both strong positive predictors of occupancy for Grace's Warbler (Z >2.00; Table 2). Vegetation type was the only "strong" predictor for Western Bluebirds with occupancy rates higher in ponderosa pine than other communities. Basal area and vegetation type, namely a negative association with ponderosa pine, were also strong predictors for Ruby-crowned Kinglets (Table 2). The quadratic form of basal area, variation in basal area or density, variation in vegetation type, and expressions of canopy cover were present in many of the best models but were not strong predictors of occupancy (Table 2).

Spatially Explicit Models of Occupancy

Our single season models of occupancy indicated affinities for environmental variables that were different for each species. Accordingly, these results were reflected in our spatially explicit models of occupancy in both 2006 and 2010. Relatively high probabilities of occupancy were predicted for Western Bluebird (Figures 7 and 8) across most of the study area. Predictions for Grace's Warbler suggested a more restricted spatial distribution in this species (Figures 3 and 4). Results for Ruby-crowned Kinglet indicated also were restricted, with areas of high occupancy predicted primarily in higher-elevation mixed-conifer forests (Figures 5 and 6). A comparison of model predictions from 2006 and 2010 depicted changes in occupancy of Grace's Warbler resulting from associated changes in forest structural attributes in the intervening years (Figure 9).

Dynamic Models of Occupancy

We generated trends in occupancy for both Grace's Warbler and Western Bluebird using multi-season occupancy models. Annual estimates of occupancy for Grace's Warbler were highest in 2006 (0.57; Figure 2), lowest in 2007 (0.41), and appeared to increase slightly between 2008 and 2009. Similarly, this species displayed annual increases in colonization while local extinction rates were similar across years (Table 3). Western Bluebird occupancy was constant or increasing throughout the analysis period (between 0.48 and 0.58; Figure 2).

Discussion

Model selection results indicated that single-season models of occupancy that included environmental covariates performed considerably better than the null model for all species. These results provide evidence that forest structural attributes likely to be impacted or manipulated by forest restoration activities can be important predictors of occupancy; however, from a bird's perspective, there likely are more biologically meaningful covariates (e.g., presence of snags) than were examined here. Models incorporating environmental covariates outperformed the null models for all species, although many of the variables

contained in the best models had *Z*-scores <2.0, indicating some degree of variable uncertainty associated with identifying the single strongest predictor of occupancy. This provides an indication that there were indeed additional biologically relevant covariates that could have been examined; however, those covariates may not be as sensitive to forest restoration treatments (e.g., slope, elevation, etc.).

Comparison of the best (in terms of AIC value) models with the null models for the less common Grace's Warbler, Ruby-crowned Kinglet, and Western Bluebird indicated that the environmental elements examined here were strongly associated with occupancy for these species. Our usage of model-averaged parameter estimates to develop continuous, spatially explicit probabilistic surfaces directly incorporated this model selection uncertainty. Additionally, given that detection probabilities varied by species, changed annually, and often were considerably less than one (Figure 1), these results can be viewed as unbiased relative to approaches that do not explicitly account for detection probability. Finally, multi-season occupancy models indicated stable trends for Western Bluebird and increasing (although variable) trends for Grace's Warbler. Small sample size in the initial years of surveys prevented evaluation of trends for Ruby-crowned Kinglet.

Grace's Warbler is typically found in xeric pine or pine-oak dominated habitats characterized by larger trees with mid-range values of canopy cover (Stacier & Guzy 2002). While we did not focus on ecologically or biologically meaningful covariates, our results indicated that both basal area and lower canopy cover were strong positive predictors of occupancy for Grace's Warbler. Planned management actions on the Kaibab National Forest that reduce canopy cover with minimal effects on basal area are likely to result in increases in predicted occupancy for Grace's Warbler.

Studies of Western Bluebird habitat have documented preferences for more open, park-like forested settings (Guinan et al. 2008; Kingery & Ghalambor 2001). While we observed a strong relationship between ponderosa pine and bluebird occupancy, few forest structural variables were strong predictors of occupancy. While planned management activities that do not result in vegetation community change are unlikely to affect bluebird occupancy, our

results indicate that some change in bluebird occupancy may result from associated changes in basal area.

Although Ruby-crowned Kinglet is not a mixed-conifer obligate (Swanson et al. 2008), the strong negative association with ponderosa pine that we observed resulted in occupancy estimates that were higher within the mixed-conifer vegetation type. The positive association with basal area and negative association with intermediate canopy cover values may also be more indicative of current conditions in mixed conifer forests. Management actions that reduce these conditions are likely to result in changes in kinglet occupancy.

Trends in occupancy for Grace's Warbler indicated an initial decline between 2006 and 2007, followed by a gradual increase in subsequent years. Western Bluebird trends were similar for the latter portion of our study, but showed a marked increase between 2006 and 2007. Caution should be used in interpreting the magnitude of these trends given the standard errors for annual estimates of occupancy for each species. Trends were not presented for the Ruby-crowned Kinglet due to the sharp change in detectability from 2006 to 2007 and insufficient sample sizes to estimate colonization and local extinction rates for the first two years of surveys.

Conclusions and Future Directions

The sampling design and resolution of the spatial data used here are intended to provide estimates of environmental relationships at mid- to landscape scales that can be used for monitoring and predicting the response of a species to future treatments and are not appropriate for identifying fine-scale habitat associations that are more appropriately evaluated using other techniques, such as territory mapping. Additional fine-scale habitat information (e.g., presence of snags, presence of large trees, etc.) could be used within a hierarchical modeling framework (e.g., Mordecai et al. 2011) to further refine the models used here and more explicitly account for the multiple scales at which songbirds are likely using habitat.

For these analyses, we generated models of occupancy for all three species relating probability of occupancy to a suite of environmental (i.e., forest structure) covariates that were

likely to be altered by forest restoration or fuels reduction treatments. The probabilistic surfaces generated using these models reflect occupancy under forest conditions in 2006 and 2010. Figure 9 illustrates a potential application of these two datasets for examining change over time, where occupancy estimates (i.e., regression coefficients) from 2006, and conditioned on forest structure layers derived for that year, are used to estimate occupancy in 2010, in turn conditioned on forest layers derived for 2010. Changes in occupancy between 2006 and 2010, or subsequent years, could be used to monitor and evaluate any landscape-scale effects of management actions on these species. In addition, these models can serve as a valuable tool for analyzing the potential effects of management actions on forests structure and wildlife in a scenario-based framework, and before these actions are implemented. For example, forest structural variables can be modified based on hypothetical forest treatments and the occupancy models re-run to determine potential treatment outcomes.

Using multi-season occupancy methods, we were able to derive trends for two of the three species of interest. Tracking these trends over time can provide land managers with valuable information regarding the cumulative impacts of ongoing management activities. Additionally, for species with small sample sizes, annual occupancy rates can be more precisely estimated than estimates of density or abundance, and may yield trend information more efficiently than alternative methods. Also, for species with sufficient sample size, environmental covariates can be related to colonization and local extinction rates to provide managers with additional information on how management activities may impact songbird occupancy dynamics.

Coarse measures of abundance or density are often used to indicate the effects of management action or environmental change on songbirds. Indeed, when species are detected imperfectly, precise and unbiased estimates of these quantities can be difficult or expensive to obtain. Occupancy estimation techniques provide a powerful and meaningful alternative to estimation or index-based techniques that do not directly account for imperfect detection, especially when the goal of a study is to quantitatively relate environmental characteristics to the response variable of interest (Zylstra et al. 2010). In addition, occupancy may be a more meaningful indicator of habitat quality as it is less subject to fluctuations in density or

abundance due to factors (e.g., changes on the wintering ground of a migratory species) unrelated to the habitat or environmental variables of interest. Conveniently, occupancy estimates can be mathematically related to estimates of abundance in situations where such information is complimentary or required (Royle & Nichols 2003).

REFERENCES

Anderson, D. R. *2008*. Model based inference in the life sciences: *a primer on evidence*. Springer, New York, NY.

Breiman, L. 2001. Random Forests. Machine Learning **45**:5-32.

Buckland, S. T., D. R. Anderson, K. P. Burnham, J. L. Laake, D. L. Borchers, and L. Thomas 2001. Introduction to distance sampling: estimating abundance of biological populations. Oxford University Press, Oxford, UK.

Burnham, K. P., and D. R. Anderson 2002. Model selection and multimodel inference: a practical information-theoretic approach. Springer-Verlag, New York, NY.

Dickson, B. G., E. Fleishman, D. S. Dobkin, and S. R. Hurteau. 2009. Relationship between avifaunal occupancy and riparian vegetation in the central Great Basin (Nevada, USA). Restoration Ecology **17**:722-730.

Guinan, J. A., P. A. Gowaty, and E. K. Eltzroth. 2008. Western Bluebird (*Sialia mexicana*). The Birds of North America Online (A. Poole, Ed.). Cornell Lab of Ornithology.

Hanni, D. J., C. M. White, J. A. Blakesley, G. J. Levandoski, and J. J. Birek. 2009. Point transect protocol. 37pp. Rocky Mountain Bird Observatory, Brighton, CO.

Kingery, H. E., and C. K. Ghalambor. 2001. Pygmy Nuthatch (*Sitta pygmaea*). The Birds of North America Online (A. Poole, Ed.). Cornell Lab of Ornithology.

MacKenzie, D. I., J. D. Nichols, J. E. Hines, M. G. Knutson, and A. B. Franklin. 2003. Estimating site occupancy, colonization, and local extinction when a species is detected imperfectly. Ecology **84**:2200-2207.

MacKenzie, D. I., J. D. Nichols, J. A. Royle, K. H. Pollock, L. L. Bailey, and J. E. Hines 2006. Occupancy estimation and modeling: Inferring patterns and dynamics of species occurrence. Academic Press, San Diego, CA.

MacKenzie, D. I., J. D. Nichols, N. Sutton, K. Kawanishi, and L. L. Bailey. 2005. Improving inferences in population studies of rare species that are detected imperfectly. Ecology **86**:1101-1113.

Mattsson, B. J., and M. R. Marshall. 2009. Occupancy modeling as a framework for designing avian monitoring programs: A case study along Appalachian streams in southern West Virgina. Pages 617 - 632 in T. D. Rich, C. Arizmendi, D. Demarest, and C. Thompson, editors. Tundra to Tropics: Connecting birds, habitats and people. Proceedings of the 4th International Partners in Flight Conference. Partners in Flight, McAllen, TX.

Mordecai, R. S., B. J. Mattsson, C. J. Tzilkowski, and R. J. Cooper. 2011. Addressing challenges when studying mobile or episodic species: hierarchical Bayes estimation of occupancy and use. Journal of Applied Ecology **48**:56-66.

Neter, J., M. H. Kutner, C. J. Nachtsheim, and W. Wasserman. 1996. Applied linear statistical models. Fourth edition. WCB/McGraw-Hill, Chicago, IL, USA.

Rosenstock, S. S., D. R. Anderson, K. M. Giesen, T. Leukering, and M. F. Carter. 2002. Landbird counting techniques: current practices and an alternative. The Auk **119**:46-53.

Royle, J. A., and J. D. Nichols. 2003. Estimating abundance from repeated presence-absence data or point counts. Ecology **84**:777-790.

Saracco, J. F., D. F. Desante, and D. R. Kaschube. 2008. Assessing landbird monitoring programs and demographic causes of population trends. Journal of Wildlife Management **72**:1665-1673.

Stacier, C. A., and M. J. Guzy. 2002. Grace's Warbler (*Dendroica graciae*). The Birds of North America Online (A. Poole, Ed.). Cornell Lab of Ornithology.

Stein Foster, V., B. Noble, K. Bratland, and R. Joos. 2010. Management Indicator Species of the Kaibab National Forest: an evaluation of population and habitat trends (version 3.0). Page 256. USDA Forest Service, Kaibab National Forest, Williams, AZ.

Swanson, D. L., J. L. Ingold, and G. E. Wallace. 2008. Ruby-crowned Kinglet (*Regulus calendula*). The Birds of North America Online (A. Poole, Ed.). Cornell Lab of Ornithology.

Zylstra, E. R., R. J. Steidl, and D. E. Swann. 2010. Evaluating survey methods for monitoring a rare vertebrate, the Sonoran Desert Tortoise. Journal of Wildlife Management **74**:1311-1318.

Table 1. Results of occupancy model selection for Grace's Warbler, Ruby-crowned Kinglet, and Western Bluebird on the Kaibab National Forest (Arizona, USA). Modeled effects (i.e., habitat variables) included basal area (BA), standard deviation of basal area (BA_SD), standard deviation of tree density (TPA_SD), variation in existing vegetation type (VarEVT), ponderosa pine vegetation type (VegPP), mixed-conifer vegetation type (VegMC) northeastern orientation (NE), and percent canopy cover (CC__). Canopy cover is expressed as "1" for all values <35% (CC35), all values ≤21.03% (CC21), or all values >21.03% and ≤46.56% (CC47). All variables were derived from digital data. Squared term indicates the quadratic form of the variable (BA^2). Null models are denoted by (.). Yearly differences in detection probability are denoted as (y). All models were conditioned on a single best model of detection probability, where *p* for Grace's Warbler, Ruby-crowned Kinglet, and Western Bluebird was a function of (y, BA, BA^2, BA_SD, TPA_SD, CC21, CC47, VegPP, VarEVT, NE), (y, BA, BA^2, BA_SD,TPA_SD, CC21, VegPP, VegMC, VarEVT, NE), and (y, BA, BA^2, BA_SD, VegPP, VarEVT, NE) respectively.

Model	K[1]	AIC[2]	ΔAIC[3]	w[4]
Grace's Warbler				
ψ(BA, BA_SD, TPA_SD, CC21, CC47, VarEVT)	20	2383.32	0.00	0.3557
ψ(BA, BA_SD, TPA_SD, CC21, CC47)	19	2383.56	0.24	0.3154
ψ(BA, BA_SD, TPA_SD, CC21, CC47, VegMC, VarEVT)	21	2384.86	1.54	0.1647
ψ(BA, TPA_SD, CC21, CC47)	18	2385.86	2.54	0.0999
ψ(BA, BA_SD, TPA_SD, CC21, CC47, VegMC, VarEVT, NE)	22	2386.74	3.42	0.0643
ψ(.)	14	2404.93	21.61	0.0000
Ruby-crowned Kinglet				
ψ(BA, TPA_SD, CC47, VegPP)	18	1400.75	0.00	0.4664
ψ(BA, BA^2, TPA_SD, CC47, VegPP)	19	1402.01	1.26	0.2484
ψ(BA, BA^2, BA_SD, TPA_SD, CC47, VegPP)	20	1403.69	2.94	0.1072
ψ(BA, CC47, VegPP)	17	1404.09	3.34	0.0878
ψ(.)	14	1427.84	27.09	0.0000
Western Bluebird				
ψ(BA, BA^2, VegPP)	15	2036.03	0.00	0.2570
ψ(BA, BA^2, CC35, VegPP)	16	2036.63	0.60	0.1904
ψ(BA, BA^2, CC35, VegPP, VegMC)	17	2037.10	1.07	0.1505
ψ(BA, BA^2, CC35, VegPP, VegMC, VarEVT)	18	2037.24	1.21	0.1404
ψ(BA, BA^2, BA_SD, CC35, VegPP, VegMC, VarEVT)	19	2037.50	1.47	0.1232
ψ(BA, BA_SD, CC35, VegPP, VegMC, VarEVT)	18	2038.61	2.58	0.0708
ψ(BA, BA^2, BA_SD, CC35, VegPP, VegMC, VarEVT, NE)	20	2039.34	3.31	0.0491
Ψ(.)	12	2048.45	12.42	0.0005

[1]Total number of model parameters, including those used to estimate *p*

[2]Akaike's Information Criterion

[3]AIC difference value

[4]AIC model weight

Table 2. Model-averaged regression coefficients $\left(\tilde{\bar{\beta}}\right)$, unconditional standard errors (SE), and Z-statistics (*Z*) for habitat variables included in the best model(s) (AIC<4.0; Table 1) of occupancy for Grace's Warbler, Ruby-crowned Kinglet, and Western Bluebird on the Kaibab National Forest (Arizona, USA). Estimates of basal area, the quadratic form of basal area, standard deviation of basal area, and standard deviation of tree density are based on standardization and rescaling of all variables prior to analysis, and conditioned on a single best model of detection probability (Table 1). Variables that were not estimated because they were absent from the best model set are denoted as "—".

	Grace's Warbler			Ruby-crowned Kinglet			Western Bluebird		
Habitat variable	$\tilde{\bar{\beta}}$	SE	*Z*[1]	$\tilde{\bar{\beta}}$	SE	*Z*[1]	$\tilde{\bar{\beta}}$	SE	*Z*[1]
Basal area	4.02	1.18	3.42	1.19	0.43	2.73	0.46	0.69	0.67
Basal area squared	—	—	—	-0.19	0.34	-0.57	-0.80	0.44	-1.80
Standard deviation of basal area	1.03	0.67	1.54	-0.04	0.11	-0.35	0.20	0.36	0.56
Standard deviation of tree density	-0.99	0.62	-1.59	0.48	0.30	1.58	—	—	—
Canopy cover (≤21.03%)	4.71	2.28	2.06	—	—	—	—	—	—
Canopy cover (21.03%<x≤46.56%)	2.41	1.20	2.01	-1.25	0.66	-1.91	—	—	—
Canopy Cover (≤35%)	—	—	—	—	—	—	0.89	1.14	0.78
Ponderosa pine vegetation type	—	—	—	-1.87	0.70	-2.67	2.39	0.95	2.52
Mixed-conifer vegetation type	0.16	0.38	0.43	—	—	—	-0.54	0.71	-0.75
Variation in vegetation type	0.26	0.38	0.67	—	—	—	0.08	0.17	0.49
Northeastern orientation	-0.02	0.08	-0.28	—	—	—	0.02	0.07	0.31
Intercept	*-3.40*	*1.65*	*-2.06*	*0.50*	*0.60*	*0.83*	*0.53*	*0.74*	*0.72*

[1]Computed as $\tilde{\bar{\beta}}/SE$

Table 3. Parameter estimates (± 1 SE) for the probability of colonization ($\hat{\gamma}$) and local extinction ($\hat{\varepsilon}$) of Grace's Warbler and Western Bluebird on the Kaibab National Forest (Arizona, USA) based on $\psi_{2006}(.)\gamma(y)\varepsilon(y)p(.)$ and $\psi_{2006}(.)\gamma(y)\varepsilon(y)p(y+BA+BA^2+BA\_SD+TPA\_SD+CC35+VegPP+VegMC+VarEVT+NE)$ respectively. Estimates for Ruby-crowned Kinglet are not presented due to failure to achieve model convergence as a result of insufficient sample size in 2007.

		Year		
Species		2007	2008	2009
Grace's Warbler	$\hat{\gamma}$	0.014 (0.060)	0.309 (0.068)	0.274 (0.064)
	$\hat{\varepsilon}$	0.290 (0.099)	0.367 (0.087)	0.244 (0.069)
Western Bluebird	$\hat{\gamma}$	0.342 (0.146)	0.317 (0.115)	0.313 (0.090)
	$\hat{\varepsilon}$	0.256 (0.162)	0.286 (0.091)	0.177 (0.072)

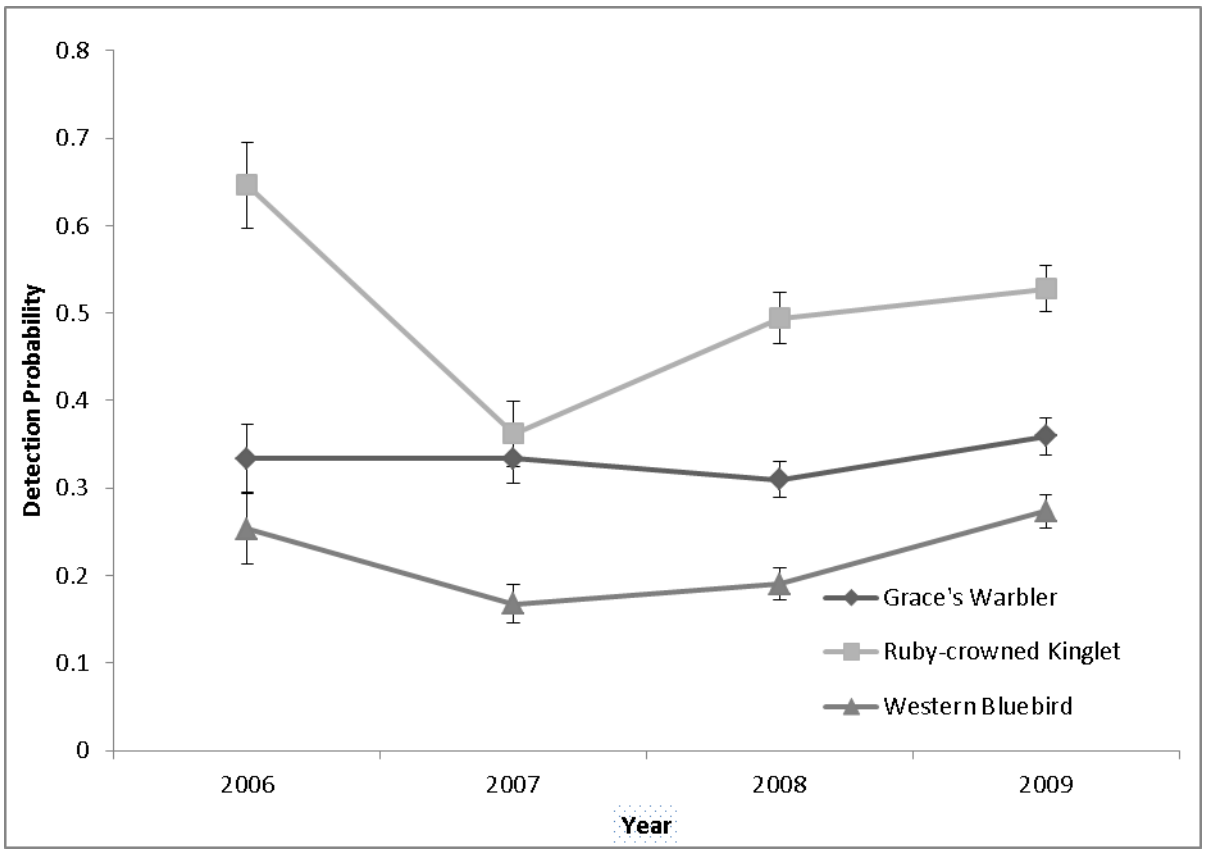

Figure 1. Annual estimates (±1 SE) of detection probability for Grace's Warbler, Ruby-crowned Kinglet, and Western Bluebird on the Kaibab National Forest (Arizona, USA). Estimates derived using: ψ_{2006}(BA+BA^2+BA_SD+TPA_SD+ CC35+VegPP+VegMC+VarEVT+ NE)γ(y+BA+BA^2+BA_SD+TPA_SD+ CC35+VegPP+VegMC+VarEVT+ NE) ε(y+BA+BA^2+BA_SD+TPA_SD+ CC35+VegPP+VegMC+VarEVT+ NE)p(y) [Grace's Warbler]; ψ_{2006}(BA+BA^2+BA_SD+TPA_SD+CC35+NE)γ(BA+BA_SD+TPA_SD+VarEVT+NE) ε(BA+BA^2 +VarEVT+NE)p(y)[Ruby-crowned Kinglet]; ψ_{2006}(BA+BA^2+BA_SD+TPA_SD+ CC35+VegPP +VarEVT+NE)γ(BA+BA^2+BA_SD+TPA_SD+CC35+VegPP+VarEVT+NE) ε(BA+BA^2 +VarEVT+NE)p(y)[Western Bluebird]. Refer to Table 1 for explanations of symbols.

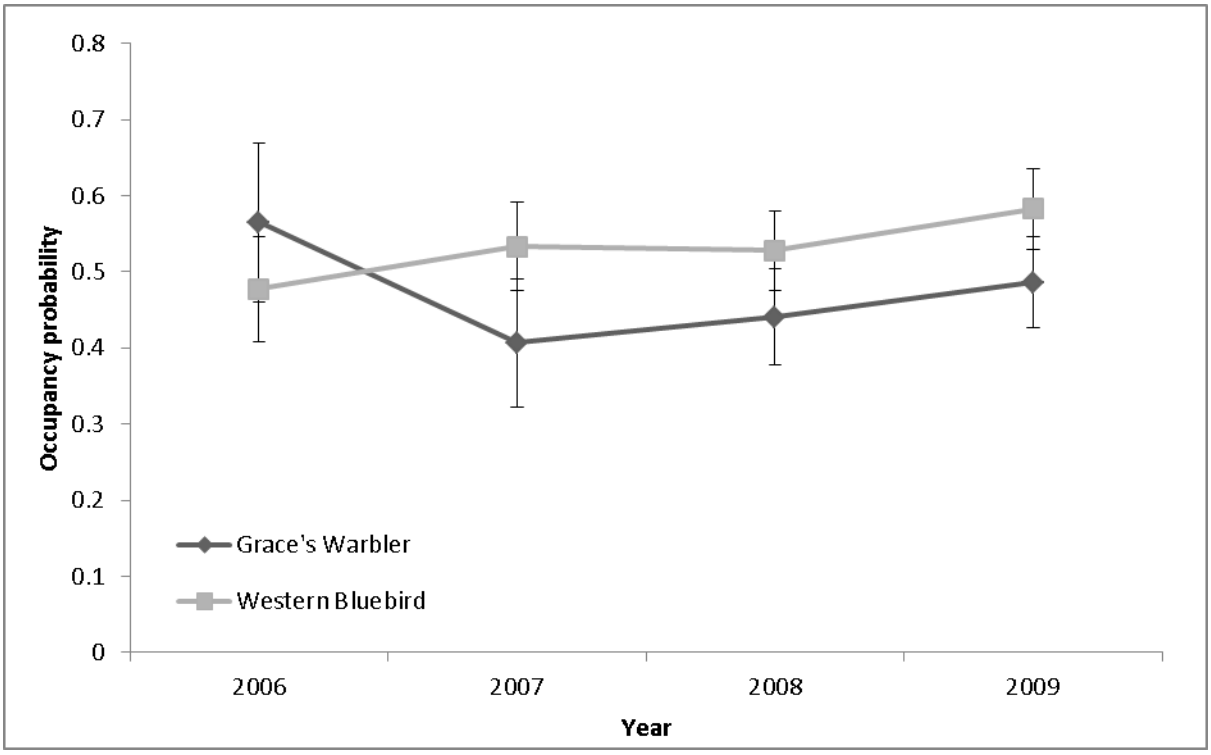

Figure 2. Annual estimates (±1 SE) of occupancy for Grace's Warbler and Western Bluebird on the Kaibab National Forest (Arizona, USA). Annual estimates for Ruby-crowned Kinglet are not presented due to failed model convergence resulting from insufficient sample size in 2007. See Table 3 for models used to derive estimates.

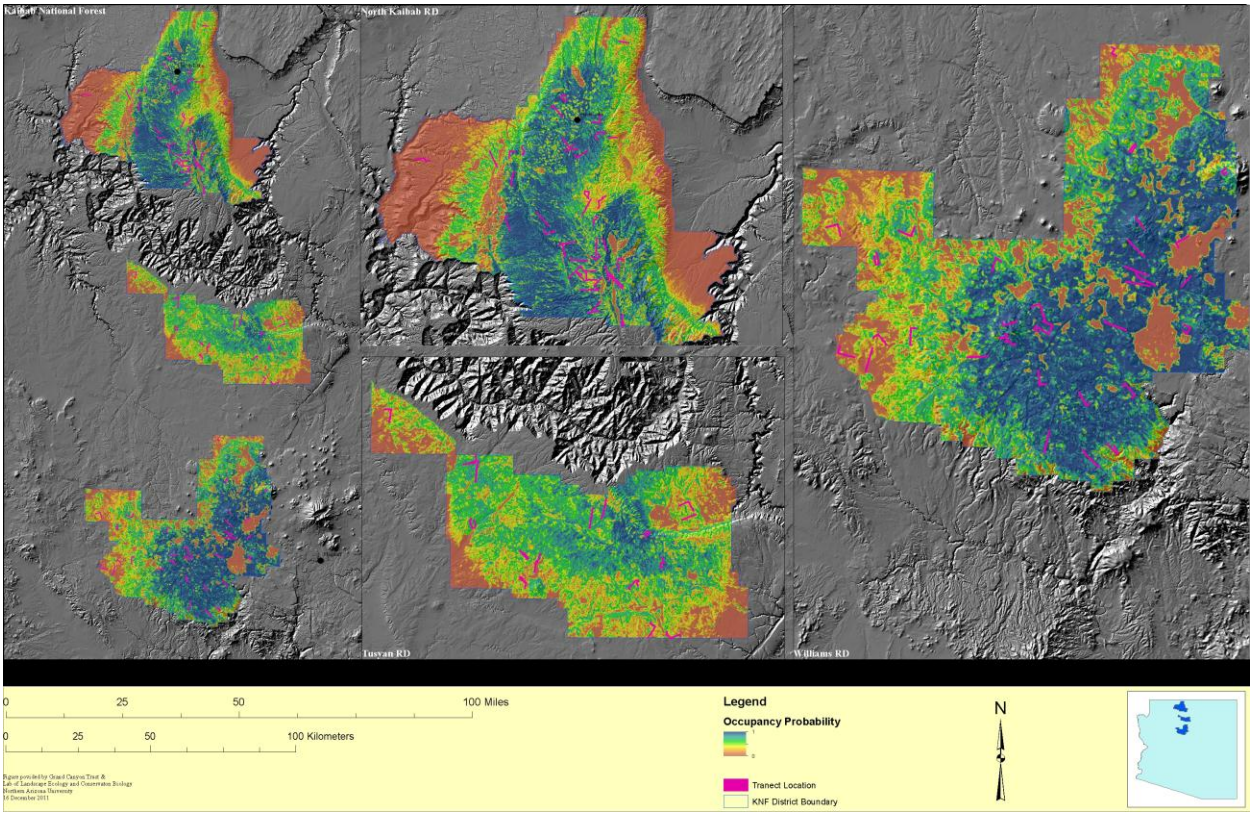

Figure 3. Spatially explicit model of Grace's Warbler occupancy on the Kaibab National Forest (Arizona, USA) in **2006**. Models of occupancy were developed using 2006 forest structural data and species observations from 2006-2009. See Table 2 for model-averaged regression coefficients used to derive this response surface. Insets detail occupancy estimates for each ranger district of the Kaibab National Forest.

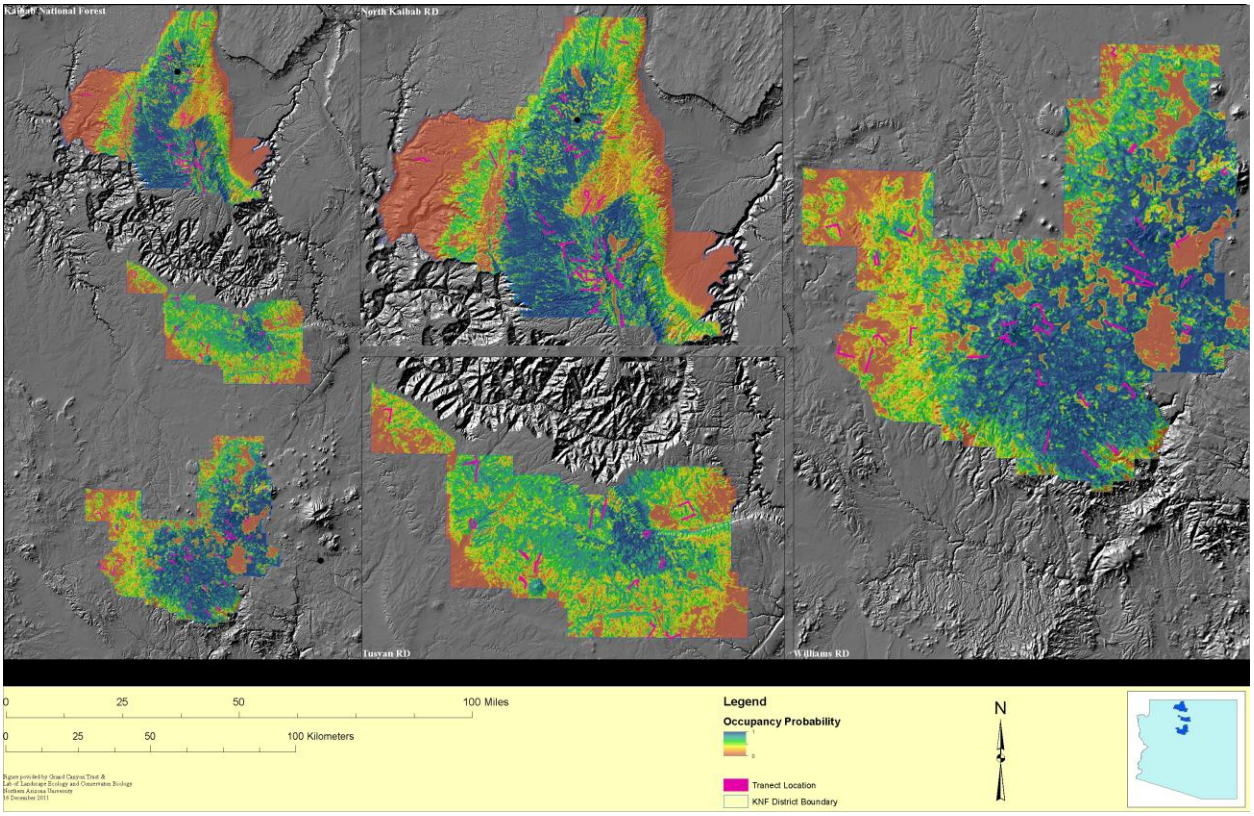

Figure 4. Spatially explicit model of Grace's Warbler occupancy on the Kaibab National Forest (Arizona, USA) in **2010**. Models of occupancy were developed using 2006 forest structural data and species observations from 2006-2009 then predicted using 2010 forest structural data. See Table 2 for model-averaged regression coefficients used to derive this response surface. Insets detail occupancy estimates for each ranger district of the Kaibab National Forest.

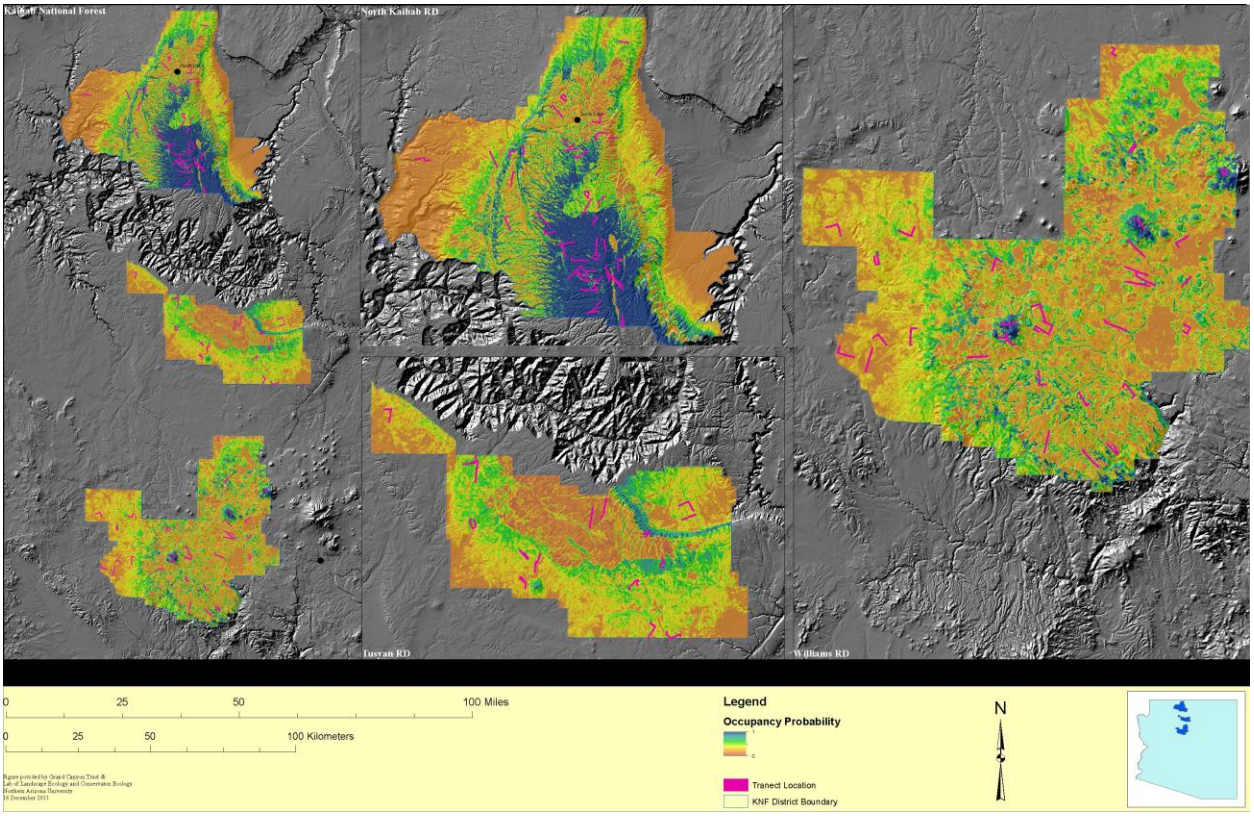

Figure 5. Spatially explicit model of Ruby-crowned Kinglet occupancy on the Kaibab National Forest (Arizona, USA) in **2006**. Models of occupancy were developed using 2006 forest structural data and species observations from 2006-2009. See Table 2 for model-averaged regression coefficients used to derive this response surface. Insets detail occupancy estimates for each ranger district of the Kaibab National Forest.

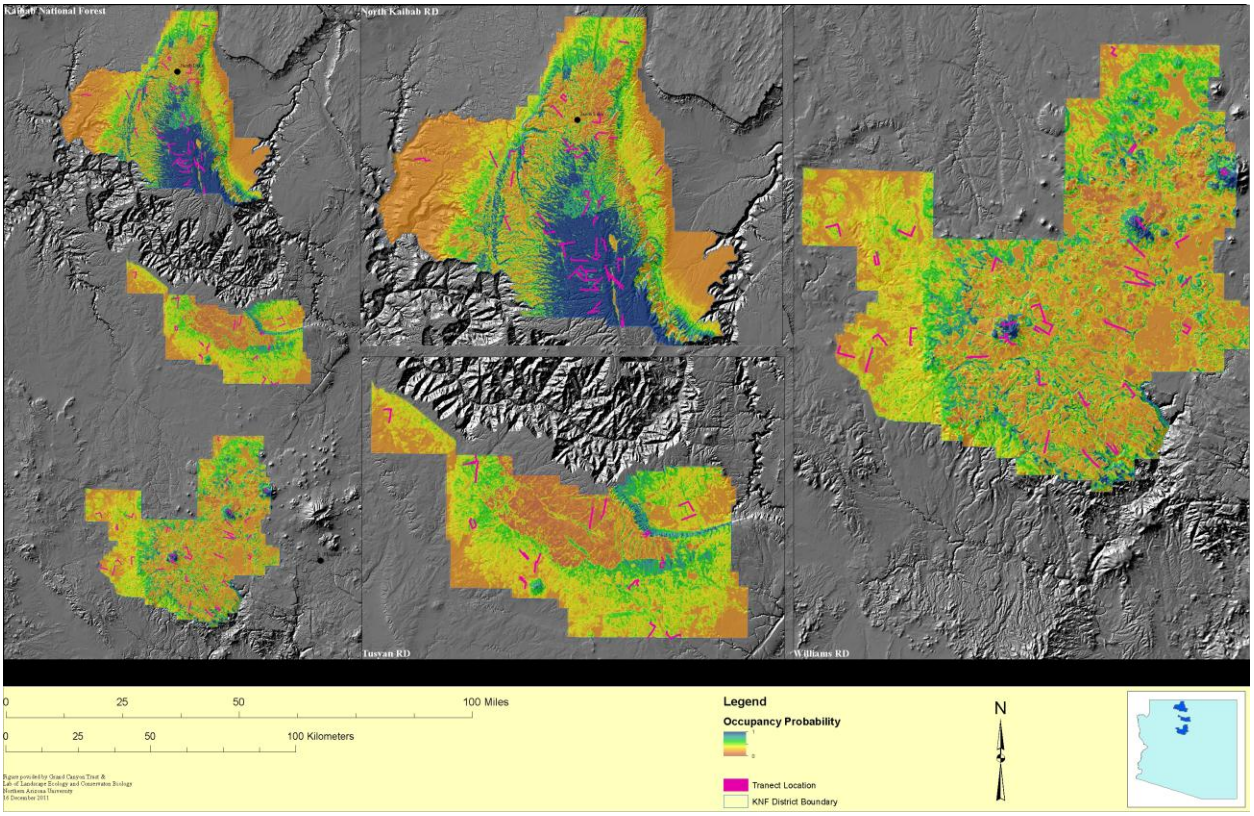

Figure 6. Spatially explicit model of Ruby-crowned Kinglet occupancy on the Kaibab National Forest (Arizona, USA) in **2010**. Models of occupancy were developed using 2006 forest structural data and species observations from 2006-2009 then predicted using 2010 forest structural data. See Table 2 for model-averaged regression coefficients used to derive this response surface. Insets detail occupancy estimates for each ranger district of the Kaibab National Forest.

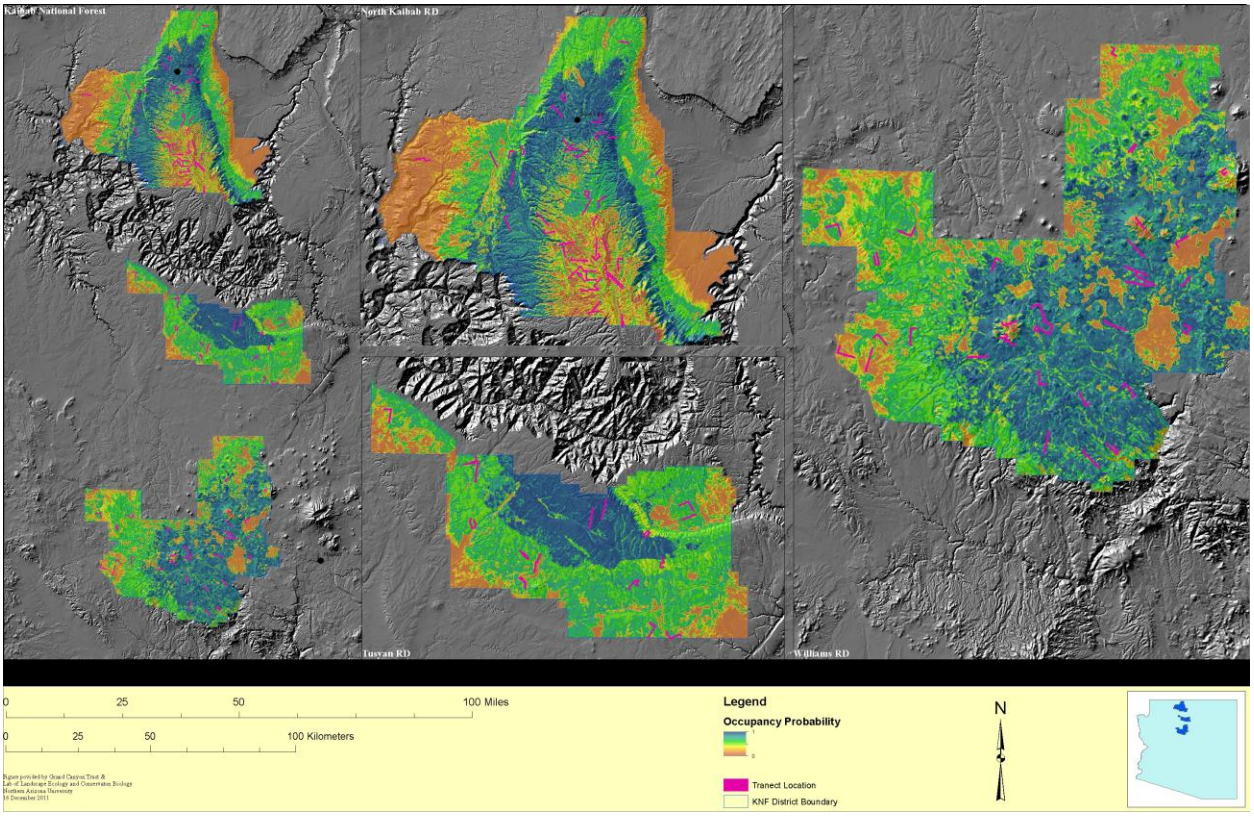

Figure 7. Spatially explicit model of Western Bluebird occupancy on the Kaibab National Forest (Arizona, USA) in **2006**. Models of occupancy were developed using 2006 forest structural data and species observations from 2006-2009. See Table 2 for model-averaged regression coefficients used to derive this response surface. Insets detail occupancy estimates for each ranger district of the Kaibab National Forest.

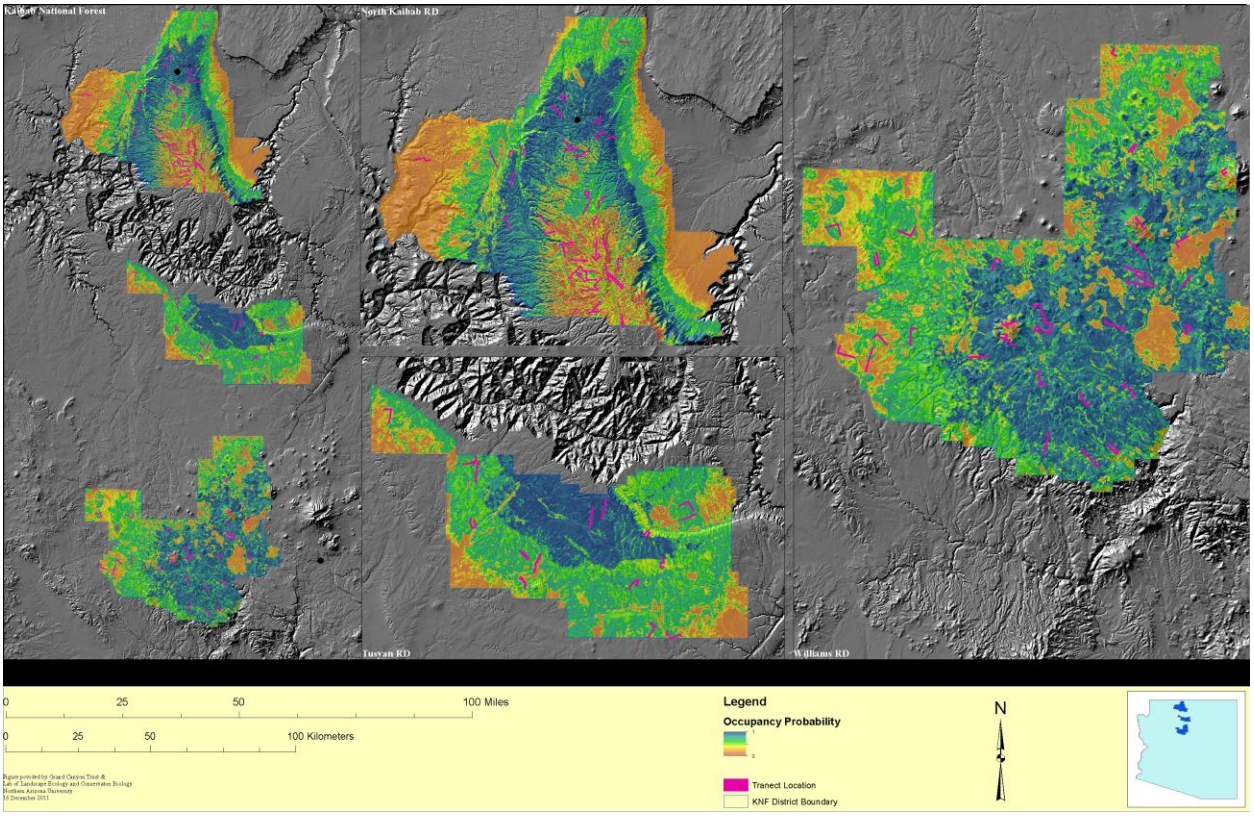

Figure 8. Spatially explicit model of Western Bluebird occupancy on the Kaibab National Forest (Arizona, USA) in **2010**. Models of occupancy were developed using 2006 forest structural data and species observations from 2006-2009 then predicted using 2010 forest structural data. See Table 2 for model-averaged regression coefficients used to derive this response surface. Insets detail occupancy estimates for each ranger district of the Kaibab National Forest.

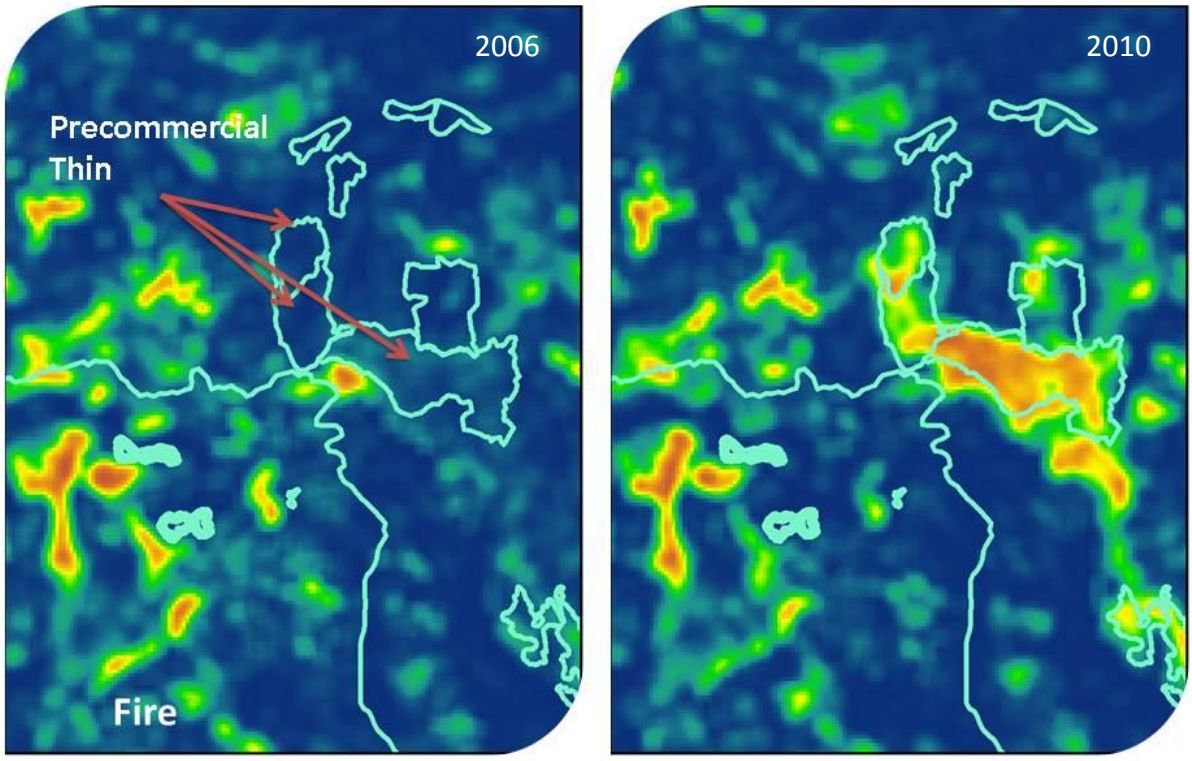

Figure 9. An example of the use of spatially explicit occupancy models for monitoring wildlife response to forest structural change. The figure displays occupancy values for Grace's Warbler within the Elk-Lee project and an adjacent fire on the Kaibab National Forest (Arizona, USA) in 2006 and 2010. Probability of occupancy decreases as colors move from blue to red (yellow is intermediate).